

# **DYNAMIC TESTING OF MGS W6X8.5 POSTS AT DECREASED EMBEDMENT**

Submitted by

Tyler L. Schmidt  
Undergraduate Research Assistant

Mario Mongiardini, Ph.D.  
Former Post-Doctoral Research Assistant

Robert W. Bielenberg, M.S.M.E., E.I.T.  
Research Associate Engineer

Karla A. Lechtenberg, M.S.M.E., E.I.T.  
Research Associate Engineer

John D. Reid, Ph.D.  
Professor

Ronald K. Faller, Ph.D., P.E.  
Research Assistant Professor  
Interim MwRSF Director

## **MIDWEST ROADSIDE SAFETY FACILITY**

Nebraska Transportation Center  
University of Nebraska-Lincoln  
130 Whittier Research Center  
2200 Vine Street  
Lincoln, Nebraska 68583-0853  
(402) 472-0965

Submitted to

## **NEBRASKA DEPARTMENT OF ROADS**

1500 Nebraska Highway 2  
Lincoln, Nebraska 68502

MwRSF Research Report No. TRP-03-271-12

December 17, 2012

## TECHNICAL REPORT DOCUMENTATION PAGE

1. Report No. TRP-03-271-12	2.	3. Recipient's Accession No.	
4. Title and Subtitle Dynamic Testing of MGS W6x8.5 Posts at Decreased Embedment		5. Report Date December 17, 2012	
		6.	
7. Author(s) Schmidt, T.L., Mongiardini, M., Bielenberg, R.W., Lechtenberg, K.A., Reid, J.D., and Faller, R.K.		8. Performing Organization Report No. TRP-03-271-12	
9. Performing Organization Name and Address Midwest Roadside Safety Facility (MwRSF) Nebraska Transportation Center University of Nebraska-Lincoln 130 Whittier Research Center 2200 Vine Street Lincoln, Nebraska 68583-0853		10. Project/Task/Work Unit No.	
		11. Contract © or Grant (G) No. SPR-P1(12)M318	
12. Sponsoring Organization Name and Address Nebraska Department of Roads 1500 Nebraska Highway 2 Lincoln, Nebraska 68502		13. Type of Report and Period Covered Final Report: 2011-2012	
		14. Sponsoring Agency Code	
15. Supplementary Notes Prepared in cooperation with U.S. Department of Transportation, Federal Highway Administration.			
16. Abstract (Limit: 200 words) The objective of this study was to evaluate and compare the energy absorption characteristics of W6x8.5 (W152x12.6) posts at a reduced embedment depth of 36 in. (914 mm) to that of the standard 40-in. (1,016-mm) embedded W6x8.5 (W152x12.6) posts used in the original Midwest Guardrail System (MGS). A total of eight dynamic component tests were performed – two tests with the 40-in. (1,016-mm) embedment depth and six with a 36-in. (914-mm) embedment depth. For two of the six 36-in. (914-mm) embedment tests, the load height was increased from 24 $\frac{3}{8}$ in. (632 mm) to 28 $\frac{3}{8}$ in. (733 mm). The posts were embedded in a highly compacted, coarse, crushed limestone material. For each test, acceleration data was used to determine the force vs. deflection and energy vs. deflection characteristics of the various post installations. Post-soil interaction forces and energy dissipation characteristics of the steel posts with a 36-in. (914-mm) embedment depth were compared to those for the steel post used in the original design of the MGS in both moderately and highly compacted soil. From these comparisons, the post with a 36-in. (914-mm) embedment depth was found to provide similar strength to that of the W6x9 (W152x13.4) steel post with a 40-in. (1,016-mm) embedment depth and installed in moderately compacted soil. In highly compacted soil, the post with a 36-in. (914-mm) embedment depth exhibited less resistance than the post with a 40-in. (1,016-mm) embedment depth. Therefore, the dynamic resistance of the W6x8.5 (W152x12.6) post with a 36-in. (914-mm) embedment was determined to provide enough resistance to be used with the MGS, which may allow a potential increase in the maximum rail mounting height of the MGS.			
17. Document Analysis/Descriptors Highway Safety, Crash Test, Roadside Appurtenances, MASH, MGS, W6x8.5 Posts, Decreased Embedment Depth, and Bogie Test		18. Availability Statement No restrictions. Document available from: National Technical Information Services, Springfield, Virginia 22161	
19. Security Class (this report) Unclassified	20. Security Class (this page) Unclassified	21. No. of Pages 72	22. Price

## **DISCLAIMER STATEMENT**

This report was completed with funding from the Federal Highway Administration, U.S. Department of Transportation. The contents of this report reflect the views and opinions of the authors who are responsible for the facts and the accuracy of the data presented herein. The contents do not necessarily reflect the official views or policies of Nebraska Department of Roads nor the Federal Highway Administration, U.S. Department of Transportation. This report does not constitute a standard, specification, regulation, product endorsement, or an endorsement of manufacturers.

## **UNCERTAINTY OF MEASUREMENT STATEMENT**

The Midwest Roadside Safety Facility (MwRSF) has determined the uncertainty of measurements for several parameters involved in standard full-scale crash testing and non-standard testing of roadside safety features. Information regarding the uncertainty of measurements for critical parameters is available upon request by the sponsor and the Federal Highway Administration. Test nos. MH-1 through MH-8 were non-certified component tests conducted for research and development purposes only.

The Independent Approving Authority (IAA) for the data contained herein was Mr. Scott Rosenbaugh, Research Associate Engineer.

## **ACKNOWLEDGEMENTS**

The authors wish to acknowledge sources that made a contribution to this project: (1) Nebraska Department of Roads for sponsoring this project and (2) MwRSF personnel for installing the posts and conducting the component tests.

Acknowledgement is also given to the following individuals who made a contribution to the completion of this research project.

### **Midwest Roadside Safety Facility**

J.C. Holloway, M.S.C.E., E.I.T., Test Site Manager  
S.K. Rosenbaugh, M.S.C.E., E.I.T., Research Associate Engineer  
A.T. Russell, B.S.B.A., Shop Manager  
K.L. Krenk, B.S.M.A., Maintenance Mechanic  
S.M. Tighe, Laboratory Mechanic  
D.S. Charroin, Laboratory Mechanic  
R.D. Julin, M.S.M.E., E.I.T., Former Graduate Research Assistant  
Undergraduate and Graduate Research Assistants

### **Nebraska Department of Roads**

Phil TenHulzen, P.E., Design Standards Engineer  
Jodi Gibson, Research Coordinator  
Mark Osborn, Design Resurfacing Unit Head  
Jim Knott, Roadway Design Division Head

### **Federal Highway Administration**

John Perry, P.E., Nebraska Division Office  
Danny Briggs, Nebraska Division Office

**TABLE OF CONTENTS**

TECHNICAL REPORT DOCUMENTATION PAGE ..... i

DISCLAIMER STATEMENT ..... ii

UNCERTAINTY OF MEASUREMENT STATEMENT ..... ii

ACKNOWLEDGEMENTS ..... iii

TABLE OF CONTENTS ..... iv

LIST OF FIGURES ..... vi

LIST OF TABLES ..... vii

1 INTRODUCTION ..... 1

    1.1 Background ..... 1

    1.2 Objective ..... 1

2 TEST CONDITIONS ..... 2

    2.1 Test Facility ..... 2

    2.2 Equipment and Instrumentation ..... 2

        2.2.1 Bogie ..... 2

        2.2.2 Accelerometers ..... 3

        2.2.3 Pressure Tape Switches ..... 4

        2.2.4 Digital Photography ..... 4

    2.3 End of Test Determination ..... 4

    2.4 Data Processing ..... 5

    2.5 Results ..... 5

3 DYNAMIC TESTING ..... 7

    3.1 Scope ..... 7

    3.2 Dynamic Testing Results ..... 10

        3.2.1 Test No. MH-1 ..... 10

        3.2.2 Test No. MH-2 ..... 13

        3.2.3 Test No. MH-3 ..... 16

        3.2.1 Test No. MH-4 ..... 19

        3.2.1 Test No. MH-5 ..... 22

        3.2.1 Test No. MH-6 ..... 25

        3.2.1 Test No. MH-7 ..... 28

        3.2.1 Test No. MH-8 ..... 31

    3.3 Summary of Dynamic Testing ..... 34

4 SUMMARY AND CONCLUSIONS ..... 47

5 REFERENCES ..... 49

6 APPENDICES ..... 50  
    Appendix A. Material Certifications ..... 51  
    Appendix B. Soil Batch Sieve Analysis ..... 53  
    Appendix C. Bogie Test Results ..... 55

## LIST OF FIGURES

Figure 1. Rigid Frame Bogie and Corrugated Beam .....	3
Figure 2. Bogie Testing Setup .....	8
Figure 3. W6x8.5 (W152x12.6) Steel Post Details.....	9
Figure 4. Force vs. Deflection and Energy vs. Deflection (DTS SLICE), Test No. MH-1 .....	11
Figure 5. Time-Sequential and Post-Impact Photographs, Test No. MH-1 .....	12
Figure 6. Force vs. Deflection and Energy vs. Deflection (DTS SLICE), Test No. MH-2 .....	14
Figure 7. Time-Sequential and Post-Impact Photographs, Test No. MH-2.....	15
Figure 8. Force vs. Deflection and Energy vs. Deflection (DTS SLICE), Test No. MH-3 .....	17
Figure 9. Time-Sequential and Post-Impact Photographs, Test No. MH-3.....	18
Figure 10. Force vs. Deflection and Energy vs. Deflection (DTS SLICE), Test No. MH-4 .....	20
Figure 11. Time-Sequential and Post-Impact Photographs, Test No. MH-4.....	21
Figure 12. Force vs. Deflection and Energy vs. Deflection (DTS SLICE), Test No. MH-5 .....	23
Figure 13. Time-Sequential and Post-Impact Photographs, Test No. MH-5.....	24
Figure 14. Force vs. Deflection and Energy vs. Deflection (DTS SLICE), Test No. MH-6 .....	26
Figure 15. Time-Sequential and Post-Impact Photographs, Test No. MH-6.....	27
Figure 16. Force vs. Deflection and Energy vs. Deflection (DTS SLICE), Test No. MH-7 .....	29
Figure 17. Time-Sequential and Post-Impact Photographs, Test No. MH-7.....	30
Figure 18. Force vs. Deflection and Energy vs. Deflection (DTS SLICE), Test No. MH-8 .....	32
Figure 19. Time-Sequential and Post-Impact Photographs, Test No. MH-8.....	33
Figure 20. Force vs. Deflection Comparison, Test Nos. MH-1 through MH-8.....	37
Figure 21. Force vs. Deflection Plots, 40 in. Embedment and 24 <sup>7</sup> / <sub>8</sub> in. Load Height .....	38
Figure 22. Force vs. Deflection Plots, 36 in. Embedment and 24 <sup>7</sup> / <sub>8</sub> in. Load Height .....	39
Figure 23. Force vs. Deflection Comparison, Test Nos. MH-1 through MH-8.....	40
Figure 24. Energy vs. Displacement Plots, 36 in. Embedment and 28 <sup>7</sup> / <sub>8</sub> in. Load Height.....	41
Figure 25. Energy vs. Displacement Plots, 40 in. Embedment and 24 <sup>7</sup> / <sub>8</sub> in. Load Height.....	42
Figure 26. Energy vs. Displacement Plots, 36 in. Embedment and 24 <sup>7</sup> / <sub>8</sub> in. Load Height.....	43
Figure 27. Energy vs. Displacement Plots, 36 in. Embedment and 28 <sup>7</sup> / <sub>8</sub> in. Load Height.....	44
Figure A-1. Post Material Certification, Test Nos. MH-1 through MH-8.....	52
Figure B-1. Soil Gradation for Test Nos. MH-1 through MH-8.....	54
Figure C-1. Test No. MH-1 Results (DTS SLICE) .....	56
Figure C-2. Test No. MH-1 Results (EDR-3).....	57
Figure C-3. Test No. MH-2 Results (DTS SLICE) .....	58
Figure C-4. Test No. MH-2 Results (EDR-3).....	59
Figure C-5. Test No. MH-3 Results (DTS SLICE) .....	60
Figure C-6. Test No. MH-3 Results (EDR-3).....	61
Figure C-7. Test No. MH-4 Results (DTS SLICE) .....	62
Figure C-8. Test No. MH-4 Results (EDR-3).....	63
Figure C-9. Test No. MH-5 Results (DTS SLICE) .....	64
Figure C-10. Test No. MH-5 Results (EDR-3).....	65
Figure C-11. Test No. MH-6 Results (DTS SLICE) .....	66
Figure C-12. Test No. MH-6 Results (EDR-3).....	67
Figure C-13. Test No. MH-7 Results (DTS SLICE) .....	68
Figure C-14. Test No. MH-7 Results (EDR-3).....	69
Figure C-15. Test No. MH-8 Results (DTS SLICE) .....	70
Figure C-16. Test No. MH-8 Results (EDR-3).....	71

**LIST OF TABLES**

Table 1. Dynamic Post Testing Matrix .....7  
Table 2. Dynamic Testing Results .....36  
Table 3. Comparison of Predicted Results to Actual Test Results .....45



## 1 INTRODUCTION

### 1.1 Background

The Midwest Guardrail System (MGS) utilizes a 6-ft (1.8-m) long, W6x8.5 (W152x12.6) steel guardrail post with an embedment depth of 40 in. (1,016 mm) and a nominal top rail mounting height of 31 in. (787 mm). The MGS has performed successfully according to the American Association of State Highway and Transportation Officials (AASHTO) *Manual for Assessing Safety Hardware* (MASH) [1] Test Level 3 (TL-3) safety performance criteria [2-4].

In order to optimize the post-soil interaction and maximize the lateral load supported by the post, it is often desirable for a steel post to rotate in the soil rather than bend and form a plastic hinge. Once the post bends under plastic deformation, the entire post is no longer rotating in the soil. Eventually, the post-soil resistance drops significantly as the steel post deforms due to lateral torsional buckling. An excessive post embedment would increase the soil resistance and reduce the capability of the entire post to rotate in the soil. On the contrary, a shallow post embedment would result in limited soil resistance during rotation and increase the propensity for the post to be removed from the ground. Therefore, it was desired to gain an understanding of the post-soil interaction characteristics associated with MGS posts with reduced embedment depths.

### 1.2 Objective

The objective of this research study was to acquire post-soil interaction data for standard W6x8.5 (W152x12.6) steel posts that may eventually allow for an increased mounting height for the MGS. As such, bogie tests were performed to determine the force vs. deflection characteristics for posts with reduced embedment depths and increased load heights. The results from this study will be used in future studies which evaluate the maximum safe guardrail mounting height for the MGS.

## 2 TEST CONDITIONS

### 2.1 Test Facility

The testing facility is located at the Lincoln Air Park on the northwest side of the Lincoln Municipal Airport and is approximately 5 miles (8.0 km) northwest of the University of Nebraska-Lincoln.

### 2.2 Equipment and Instrumentation

Equipment and instrumentation utilized to collect and record data during the dynamic bogie tests included a bogie, onboard accelerometers, pressure tape switches, high-speed and standard-speed digital video cameras, and a still camera.

#### 2.2.1 Bogie

A rigid frame bogie was used to impact the posts. A variable height, detachable impact head was used in the testing. The bogie head was constructed of 8-in. (203-mm) diameter, ½-in. (13-mm) thick standard steel pipe, with ¾-in. (19-mm) neoprene belting wrapped around the pipe to prevent local damage to the post from the impact. The impact head was bolted to the bogie vehicle, creating a rigid frame with an impact height of 24<sup>7</sup>/<sub>8</sub> in. (632 mm) or 28<sup>7</sup>/<sub>8</sub> in. (733 mm). The bogie with the impact head is shown in Figure 1. The weight of the bogie with the addition of the mountable impact head and accelerometers was 1,745 lb (792 kg) for test nos. MH-1 through MH-3 and 1,875 (850 kg) for test nos. MH-4 through MH-8.

The tests were conducted using a steel corrugated beam guardrail to guide the tire of the bogie vehicle, as shown in Figure 1. A pickup truck was used to push the bogie vehicle to the required impact velocity. After reaching the target velocity, the push vehicle braked allowing the bogie to be free rolling as it came off the track. A remote braking system was installed on the bogie allowing it to be brought safely to rest after the test.

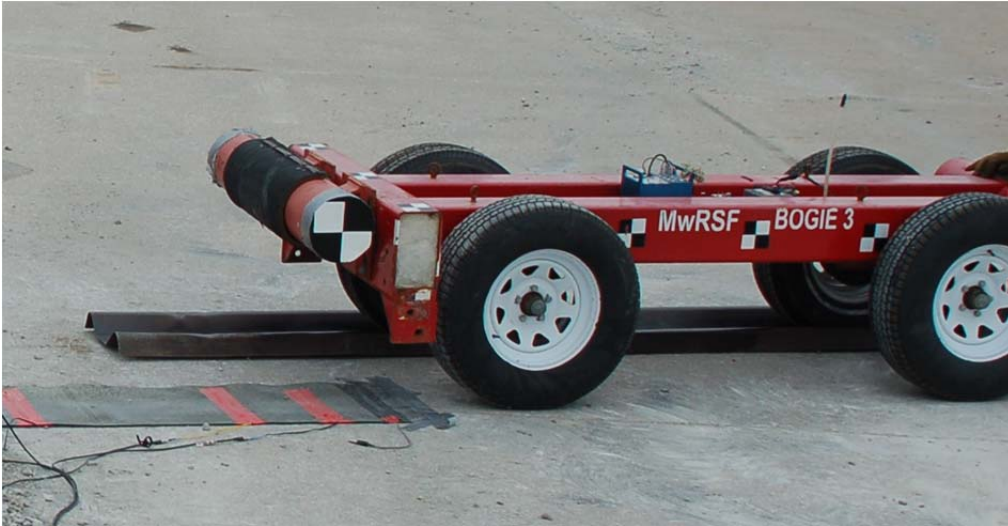


Figure 1. Rigid Frame Bogie and Corrugated Beam

### 2.2.2 Accelerometers

Two accelerometers were mounted on the bogie vehicle near its center of gravity (c.g.) to measure the acceleration in the longitudinal, lateral, and vertical directions. However, only the longitudinal accelerations were processed and reported.

The first system, SLICE 6DX, was a modular data acquisition system manufactured by DTS of Seal Beach, California. The acceleration sensors were mounted inside the body of the custom built SLICE 6DX event data recorder and recorded data at 10,000 Hz to the onboard microprocessor. The SLICE 6DX was configured with 7 GB of non-volatile flash memory, a range of  $\pm 500$  g's, a sample rate of 10,000 Hz, and a 1,650 Hz (CFC 1000) anti-aliasing filter. The "SLICEWare" computer software programs and a customized Microsoft Excel worksheet were used to analyze and plot the accelerometer data.

The second accelerometer, Model EDR-3, was a triaxial piezoresistive accelerometer system developed by IST of Okemos, Michigan. The EDR-3 was configured with 256 kB of RAM, a range of  $\pm 200$  g's, a sample rate of 3,200 Hz, and a 1,120-Hz low-pass filter. The

“DynaMax 1 (DM-1)” computer software program and a customized Microsoft Excel worksheet were used to analyze and plot the accelerometer data.

### **2.2.3 Pressure Tape Switches**

Three pressure tape switches, spaced at approximately 3.3-ft (1-m) intervals and placed near the end of the bogie track, were used to determine the speed of the bogie before impact. As the left-front tire of the bogie passed over each tape switch, a strobe light was fired sending an electronic timing signal to the data acquisition system. The system recorded the signals and the time each occurred. The speed was then calculated using the spacing between the sensors and the time between the signals. Strobe lights and high-speed digital video analysis are used only as a backup in the event that vehicle speeds cannot be determined from the electronic data.

### **2.2.4 Digital Photography**

One AOS VITcam high-speed digital video camera and two JVC digital video cameras were used to document each test. The AOS high-speed camera had a frame rate of 500 frames per second and the JVC digital video cameras had frame rates of 29.97 frames per second. The high-speed digital video camera and one digital video camera were placed laterally from the post, with a view perpendicular to the bogie’s direction of travel. The second digital video camera was placed on the opposite side of the post with respect to the other two cameras. A Nikon D50 digital still camera was also used to document pre- and post-test conditions for all tests.

## **2.3 End of Test Determination**

When the impact head initially contacted the test article, the force exerted by the surrogate test vehicle was directly perpendicular. However, as the post rotated, the surrogate test vehicle’s orientation and path moved further from perpendicular. This introduced two sources of error: (1) the contact force between the impact head and the post has a vertical component and

(2) the impact head slides upward along the test article. Therefore, only the initial portion of the accelerometer trace may be used since variations in the data become significant as the system rotates and the surrogate test vehicle overrides the system. For this reason, the end of the test needed to be defined.

Guidelines were established to define the end-of-test time using the high-speed digital video of the crash test. The first occurrence of any one of the following three events was used to determine the end of the test: (1) the test article fractures; (2) the surrogate vehicle overrides/loses contact with the test article; or (3) a maximum post rotation of 45 degrees.

## **2.4 Data Processing**

The electronic accelerometer data obtained in dynamic testing was filtered using the SAE Class 60 Butterworth filter conforming to the SAE J211/1 specifications [5]. The pertinent acceleration signal was extracted from the bulk of the data signals. The processed acceleration data was then multiplied by the mass of the bogie to get the impact force using Newton's Second Law. Next, the acceleration trace was integrated to find the change in velocity versus time. Initial velocity of the bogie, calculated from the pressure tape switch data, was then used to determine the bogie velocity, and the calculated velocity trace was integrated to find the bogie's displacement, which is also the deflection of the post. Combining the previous results, a force vs. deflection curve was plotted for each test. Finally, integration of the force vs. deflection curve provided the energy vs. deflection curve for each test.

## **2.5 Results**

The information desired from the bogie tests was the relation between the applied force and deflection of the post at the impact location. This data was then used to find the total energy (the area under the force versus deflection curve) dissipated during each test. The energy curve was used to compute the average force at a specific deflection using the following formula:

$$\bar{F} = \frac{Energy}{Deflection}$$

Although the acceleration data was applied to the impact location, the data came from the c.g. of the bogie. Error was added to the data since the bogie was not perfectly rigid and sustained vibrations. The bogie may have also rotated during impact, causing differences in accelerations between the bogie center of mass and the bogie impact head. While these issues may affect the data, the data was still valid. Filtering procedures were applied to the data to smooth out vibrations, and the rotations of the bogie during test were minor. Significant pitch angles did develop late in test no. MH-1 and MH-4 as the bogie overrode the posts; however, this occurred after the post-bogie interaction of interest. In test nos. MH-2, MH-3, and MH-5 through MH-8 the bogie ran over the post and pitching was insignificant. One useful aspect of using accelerometer data was that it included influences of the post inertia on the reaction force. This was important as the mass of the post would affect barrier performance as well as test results.

The accelerometer data for each test was processed in order to obtain acceleration, velocity, and deflection curves, as well as force vs. deflection and energy vs. deflection curves. The values described herein were calculated from the DTS SLICE data curves.

### 3 DYNAMIC TESTING

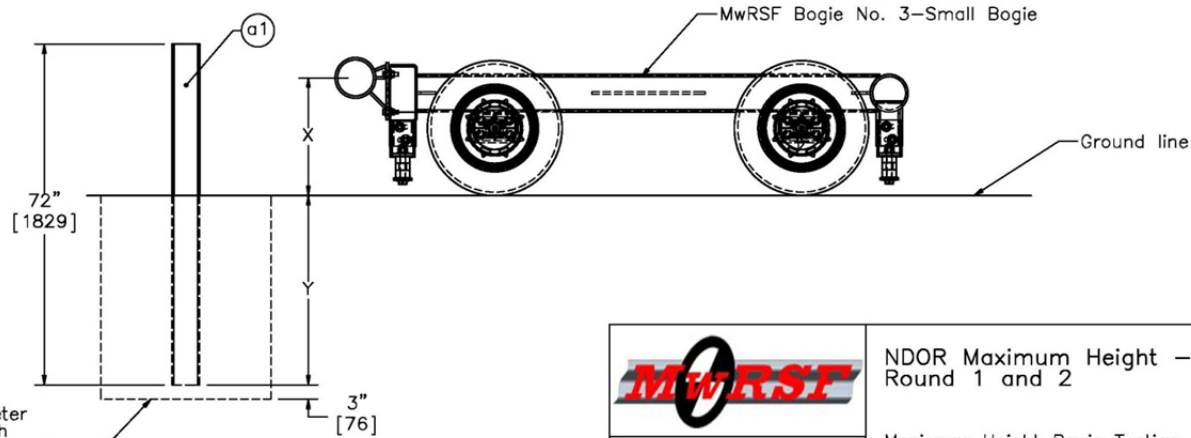
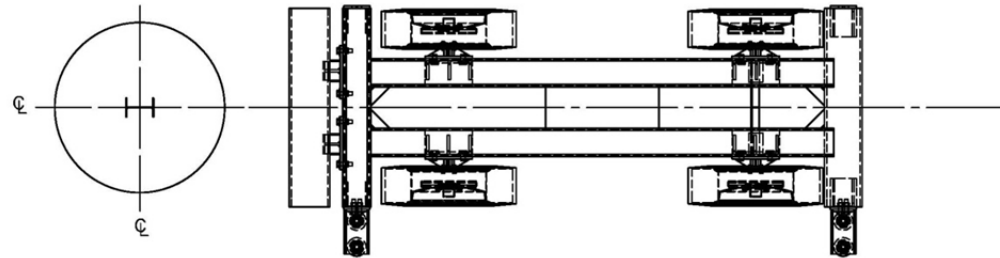
#### 3.1 Scope

Eight dynamic component tests were conducted on the W6x8.5 (W152x12.6) steel post at two different embedment depths. The target impact speed was 20 mph (32.2 km/h) for all eight tests. The target impact angle for all tests was 0 degrees, creating a classical “head-on” or full frontal impact. Six of the tests were impacted 24<sup>7</sup>/<sub>8</sub> in. (632 mm) above the ground line while the final two tests were impacted 28<sup>7</sup>/<sub>8</sub> in. (733 mm) above the ground line. The dynamic component test matrix is shown in Table 1. The test setup and W6x8.5 (W152x12.6) steel post are shown in Figures 2 and 3, respectively. Material specifications, mill certifications, and certificates of conformity for the post materials used in all eight tests are shown in Appendix A.

Table 1. Dynamic Post Testing Matrix

Test No.	Post Type	Post Length in. (mm)	Embedment Depth in. (mm)	Impact Axis	Target Impact Velocity mph(km/h)	Impact Height in. (mm)
MH-1	W6x8.5 (W152x12.6)	72 (1,829)	40 (1,016)	Strong Axis	20 (32)	24 <sup>7</sup> / <sub>8</sub> (632)
MH-2	W6x8.5 (W152x12.6)	72 (1,829)	36 (914)	Strong Axis	20 (32)	24 <sup>7</sup> / <sub>8</sub> (632)
MH-3	W6x8.5 (W152x12.6)	72 (1,829)	36 (914)	Strong Axis	20 (32)	24 <sup>7</sup> / <sub>8</sub> (632)
MH-4	W6x8.5 (W152x12.6)	72 (1,829)	40 (1,016)	Strong Axis	20 (32)	24 <sup>7</sup> / <sub>8</sub> (632)
MH-5	W6x8.5 (W152x12.6)	72 (1,829)	36 (914)	Strong Axis	20 (32)	24 <sup>7</sup> / <sub>8</sub> (632)
MH-6	W6x8.5 (W152x12.6)	72 (1,829)	36 (914)	Strong Axis	20 (32)	24 <sup>7</sup> / <sub>8</sub> (632)
MH-7	W6x8.5 (W152x12.6)	72 (1,829)	36 (914)	Strong Axis	20 (32)	28 <sup>7</sup> / <sub>8</sub> (733)
MH-8	W6x8.5 (W152x12.6)	72 (1,829)	36 (914)	Strong Axis	20 (32)	28 <sup>7</sup> / <sub>8</sub> (733)

Test Quantity	Post Type	Load Height 'X' in. [mm]	Embedment Depth 'Y' in. [mm]	Bogie No.	Impact Speed mph [km/h]
2	W6x8.5 [W150x12.6]	24 7/8 [632]	40 [1016]	3	20 [32.2]
4	W6x8.5 [W150x12.6]	24 7/8 [632]	36 [914]	3	20 [32.2]
2	W6x8.5 [W150x12.6]	28 7/8 [733]	36 [914]	3	20 [32.2]



3'-0" [914] Diameter Augered Hole with AASHTO M147-65 Grade B compacted soil or acceptable alternative

 <b>Midwest Roadside Safety Facility</b>	<b>NDOR Maximum Height - Round 1 and 2</b>	SHEET: 1 of 2
	<b>Maximum Height Bogie Testing</b>	DATE: 7/5/2012
DWG. NAME: NDOR_max_height_round1&2_R2	SCALE: 1:32 UNITS: in,[mm]	DRAWN BY: CWP
		REV. BY: KAL

Figure 2. Bogie Testing Setup



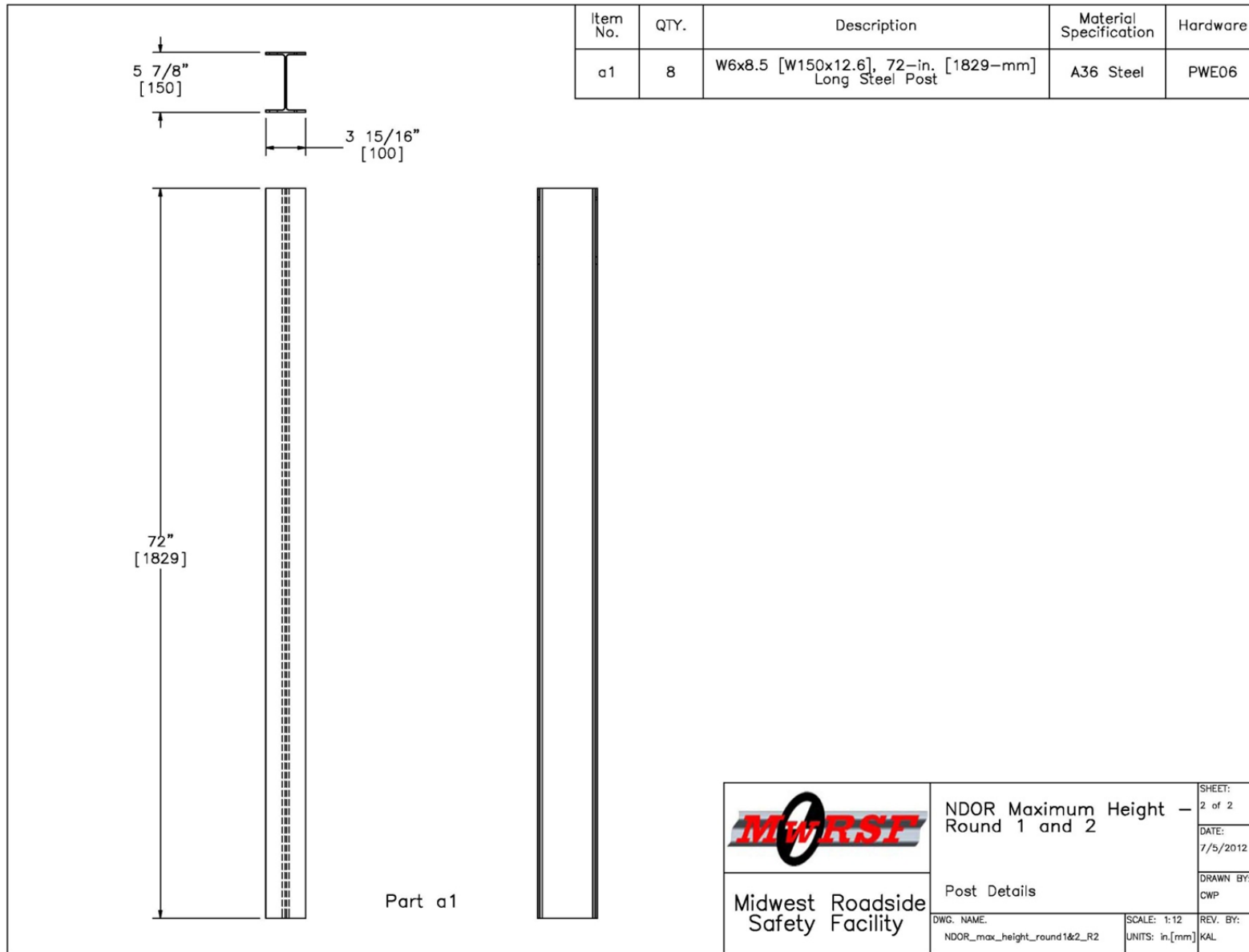


Figure 3. W6x8.5 (W152x12.6) Steel Post Details

A compacted, coarse, crushed limestone material, as recommended by MASH, was utilized for all tests [1]. Soil specifications are shown in Appendix B. MASH adheres to the general philosophy that testing longitudinal barriers in stiff soil results in higher impact and barrier loads, increased occupant risk values, and increased propensity for rail rupture, pocketing, and snag. Therefore, MASH has established a minimum post-soil resistance force standard to ensure systems are installed in strong, stiff soil. Thus, using heavily compacted soils was justified by MASH. Therefore, all tests utilized heavily compacted soil.

### **3.2 Dynamic Testing Results**

Results of each test are discussed in the following sections. Individual results for all accelerometers used during each test are provided in Appendix C.

#### **3.2.1 Test No. MH-1**

During test no. MH-1, the bogie impacted the W6x8.5 (W152x12.6) steel post with a 40-in. (1,017-mm) embedment depth at a speed of 20.8 mph (33.5 km/h). As a result the post rotated through the soil. The bogie vehicle overrode the post at a maximum displacement of 36.3 in. (922 mm). The post bent backward and yielded approximately 10 in. (254 mm) below the ground line.

Force vs. deflection and energy vs. deflection curves created from the DTS SLICE accelerometer data are shown in Figure 4. The forces quickly rose to a peak force of 14.0 kips (62.3 kN) over the first few inches of deflection. The post provided an average resistance force of around 8.8 kips (39.1 kN) through 20 in. (508 mm) of deflection. The energy absorbed by the post was 179.4 kip-in. (20.3 kJ) through 20 in. (508 mm) of deflection, and 230.6 kip-in. (26.1 kJ) through 36.3 in. (922 mm) of deflection, which corresponds to the end-of-test displacement. Time-sequential and post-impact photographs are shown in Figure 5.

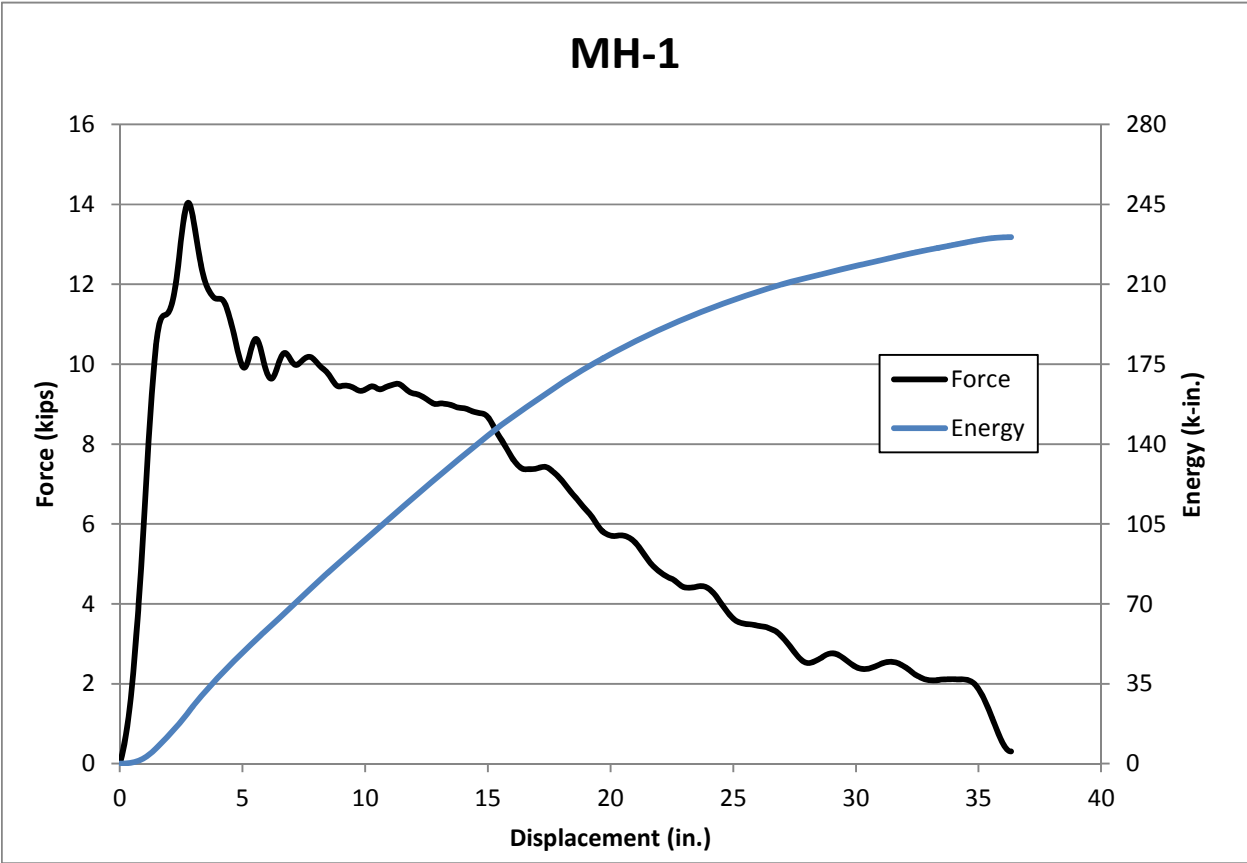
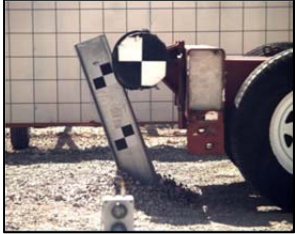


Figure 4. Force vs. Deflection and Energy vs. Deflection (DTS SLICE), Test No. MH-1



IMPACT



0.050 sec



0.100 sec



0.150 sec



0.200 sec



0.250 sec



Figure 5. Time-Sequential and Post-Impact Photographs, Test No. MH-1

### **3.2.2 Test No. MH-2**

During test no. MH-2, the bogie impacted the W6x8.5 (W152x12.6) steel post with a 36-in. (914-mm) embedment depth at a speed of 20.8 mph (33.5 km/h). As a result, the post rotated through the soil. No deformation of the post occurred. The bogie vehicle overrode the post at a maximum displacement of 36.7 in. (932 mm) as determined from the accelerometer data.

Force vs. deflection and energy vs. deflection curves created from the DTS SLICE accelerometer data are shown in Figure 6. The forces quickly rose to a peak force of 11.5 kips (51.2 kN) over the first few inches of deflection. The post provided an average resistance force of around 7.0 kips (31.1 kN) through 20 in. (508 mm) of deflection. The energy absorbed by the posts was 142.8 kip-in. (16.1 kJ) through 20 in. (508 mm) of deflection, and 165.9 kip-in. (18.7 kJ) of energy through 36.7 in. (932 mm) of deflection, which corresponds to the end-of-test displacement. Time-sequential post-impact photographs are shown in Figure 6.

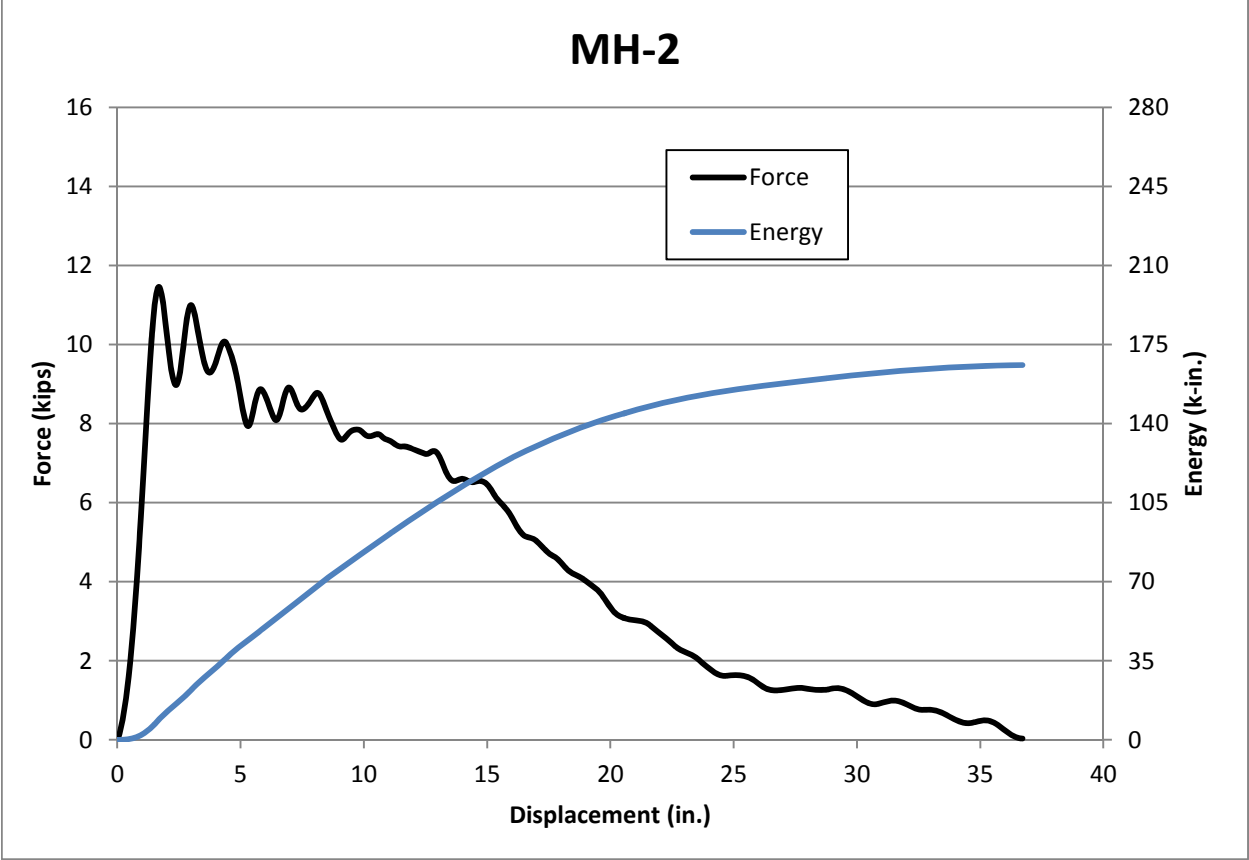
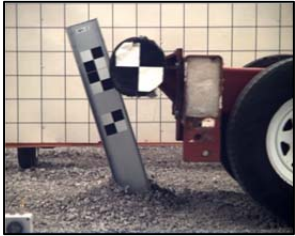


Figure 6. Force vs. Deflection and Energy vs. Deflection (DTS SLICE), Test No. MH-2





IMPACT



0.050 sec



0.100 sec



0.150 sec



0.200 sec



0.250 sec



Figure 7. Time-Sequential and Post-Impact Photographs, Test No. MH-2

### **3.2.3 Test No. MH-3**

During test no. MH-3, the bogie impacted the W6x8.5 (W152x12.6) steel post with a 36-in. (914-mm) embedment depth at a speed of 21.7 mph (34.9 km/h). As a result, the post rotated through the soil. No deformation of the post occurred. The bogie vehicle overrode the post at a maximum displacement of 39.5 in. (1,003 mm) as determined from the accelerometer data.

Force vs. deflection and energy vs. deflection curves created from the DTS SLICE accelerometer data are shown in Figure 8. The forces quickly rose to a peak force of 11.6 kips (51.6 kN) over the first few inches of deflection. The post provided an average resistance force of around 8.3 kips (36.9 kN) through 20 in. (508 mm) of deflection. The energy absorbed by the posts was 166.3 kip-in. (18.8 kJ) through 20 in. (508 mm) of deflection, and 214.3 kip-in. (24.2 kJ) of energy through 39.5 in. (1,003 mm) of deflection, which corresponds to the end-of-test displacement. Time-sequential and post-impact photographs are shown in Figure 9.



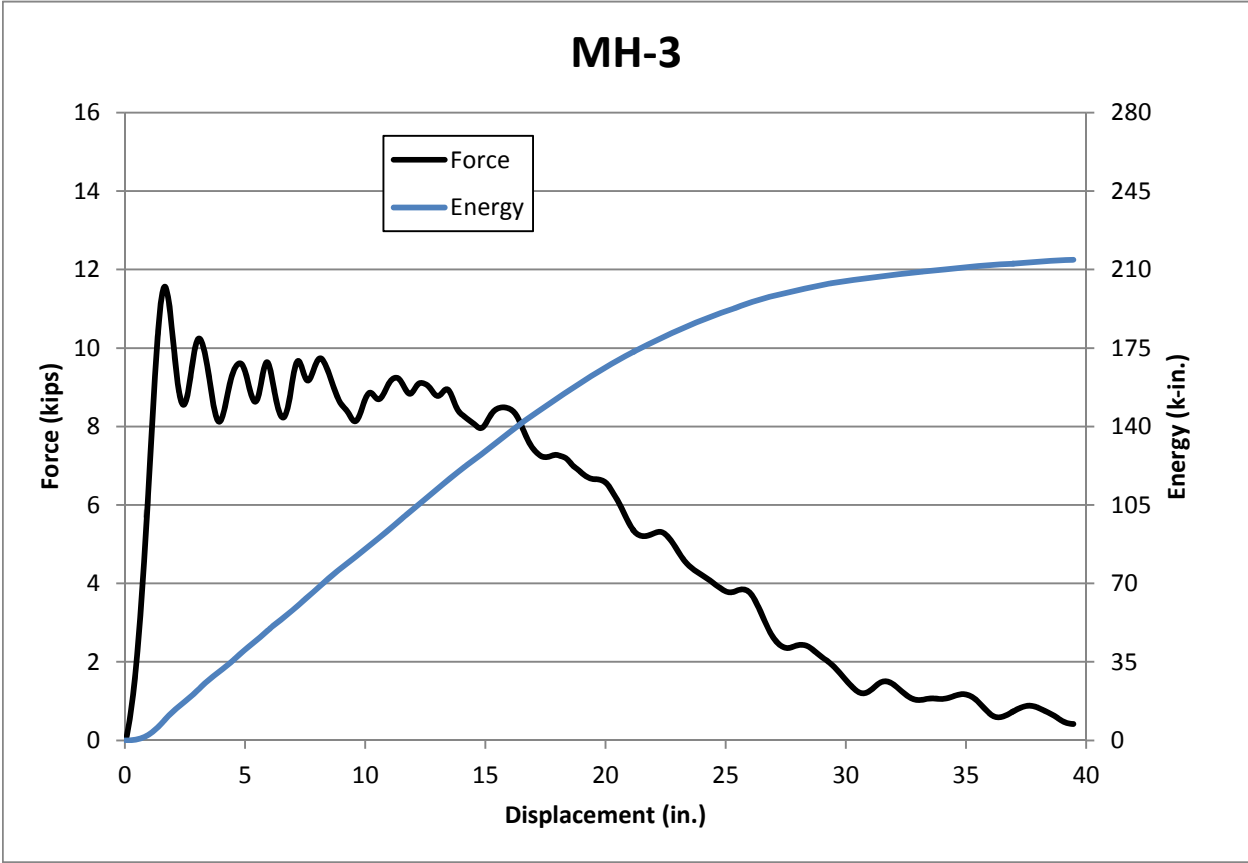


Figure 8. Force vs. Deflection and Energy vs. Deflection (DTS SLICE), Test No. MH-3



IMPACT



0.050 sec



0.100 sec



0.150 sec



0.200 sec



0.250 sec



Figure 9. Time-Sequential and Post-Impact Photographs, Test No. MH-3

### **3.2.1 Test No. MH-4**

During test no. MH-4, the bogie impacted the W6x8.5 (W152x12.6) steel post with a 40-in. (1,016-mm) embedment depth at a speed of 20.5 mph (33.0 km/h). As a result the post rotated through the soil. The bogie vehicle overrode the post at a maximum displacement of 39.0 in. (991 mm). The post bent backward and yielded approximately 10 in. (254 mm) below the ground line.

Force vs. deflection and energy vs. deflection curves created from the DTS SLICE accelerometer data are shown in Figure 10. The forces quickly rose to a peak force of 12.9 kips (57.4 kN) over the first few inches of deflection. The post provided an average resistance force of around 8.9 kips (39.6 kN) through 20 in. (508 mm) of deflection. The energy absorbed by the post was 178.5 kip-in. (20.2 kJ) through 20 in. (508 mm) of deflection, and 230.7 kip-in. (26.1 kJ) through 39.0 in. (991 mm) of deflection, which corresponds to the end-of-test displacement. Time-sequential and post-impact photographs are shown in Figure 11.

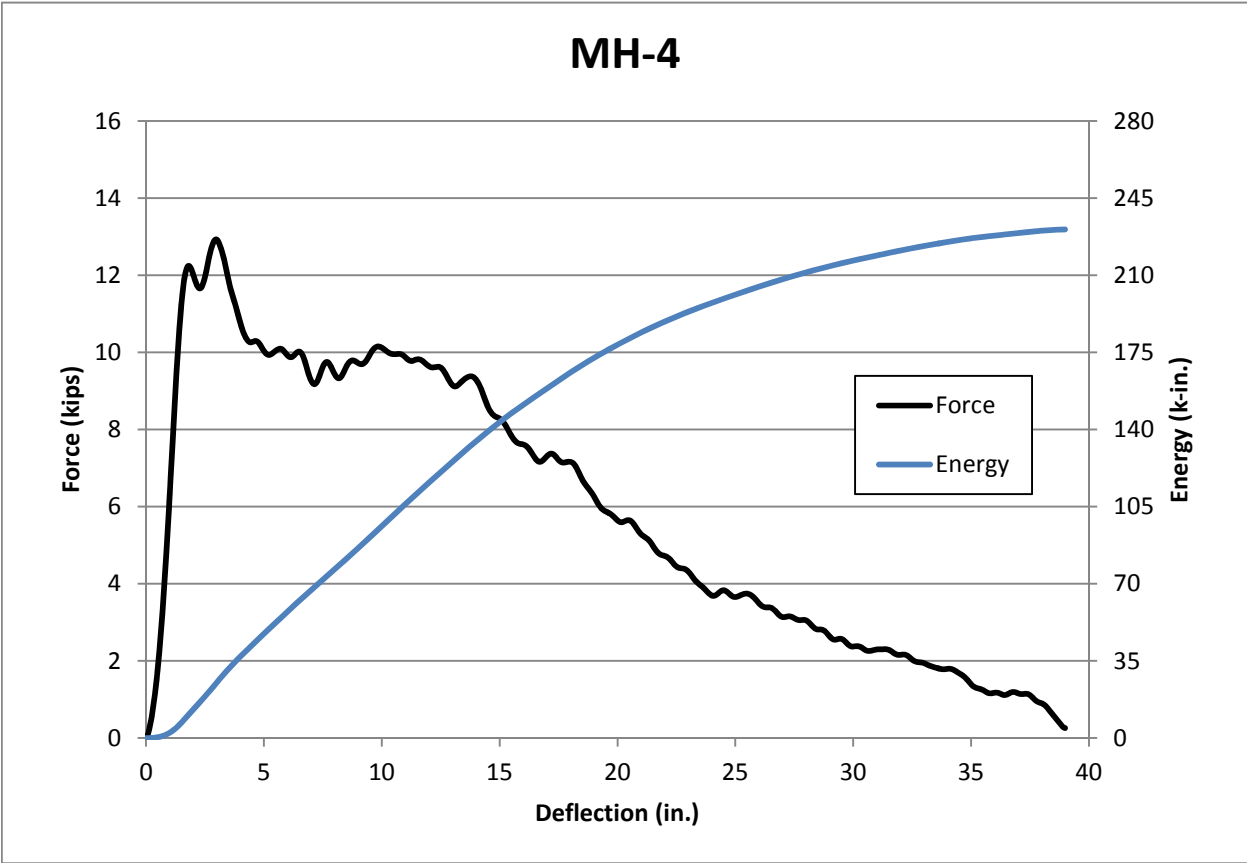
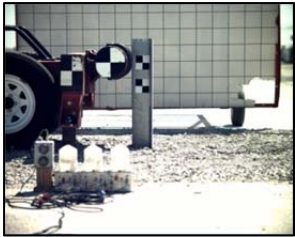


Figure 10. Force vs. Deflection and Energy vs. Deflection (DTS SLICE), Test No. MH-4





IMPACT



0.150 sec



0.300 sec



0.450 sec



0.600 sec



0.750 sec



Figure 11. Time-Sequential and Post-Impact Photographs, Test No. MH-4

### 3.2.1 Test No. MH-5

During test no. MH-5, the bogie impacted the W6x8.5 (W152x12.6) steel post with a 36-in. (914-mm) embedment depth at a speed of 19.9 mph (32.0 km/h). As a result the post rotated through the soil. No deformation of the post occurred. The bogie vehicle overrode the post at a maximum displacement of 36.8 in. (935 mm) as determined from the accelerometer data.

Force vs. deflection and energy vs. deflection curves created from the DTS SLICE accelerometer data are shown in Figure 12. The forces quickly rose to a peak force of 12.2 kips (54.3 kN) over the first few inches of deflection. The post provided an average resistance force of around 7.7 kips (34.3 kN) through 20 in. (508 mm) of deflection. The energy absorbed by the post was 153.4 kip-in. (17.3 kJ) through 20 in. (508 mm) of deflection, and 177.8 kip-in. (20.1 kJ) through 36.8 in. (935 mm) of deflection, which corresponds to the end-of-test displacement. Time-sequential and post-impact photographs are shown in Figure 13.

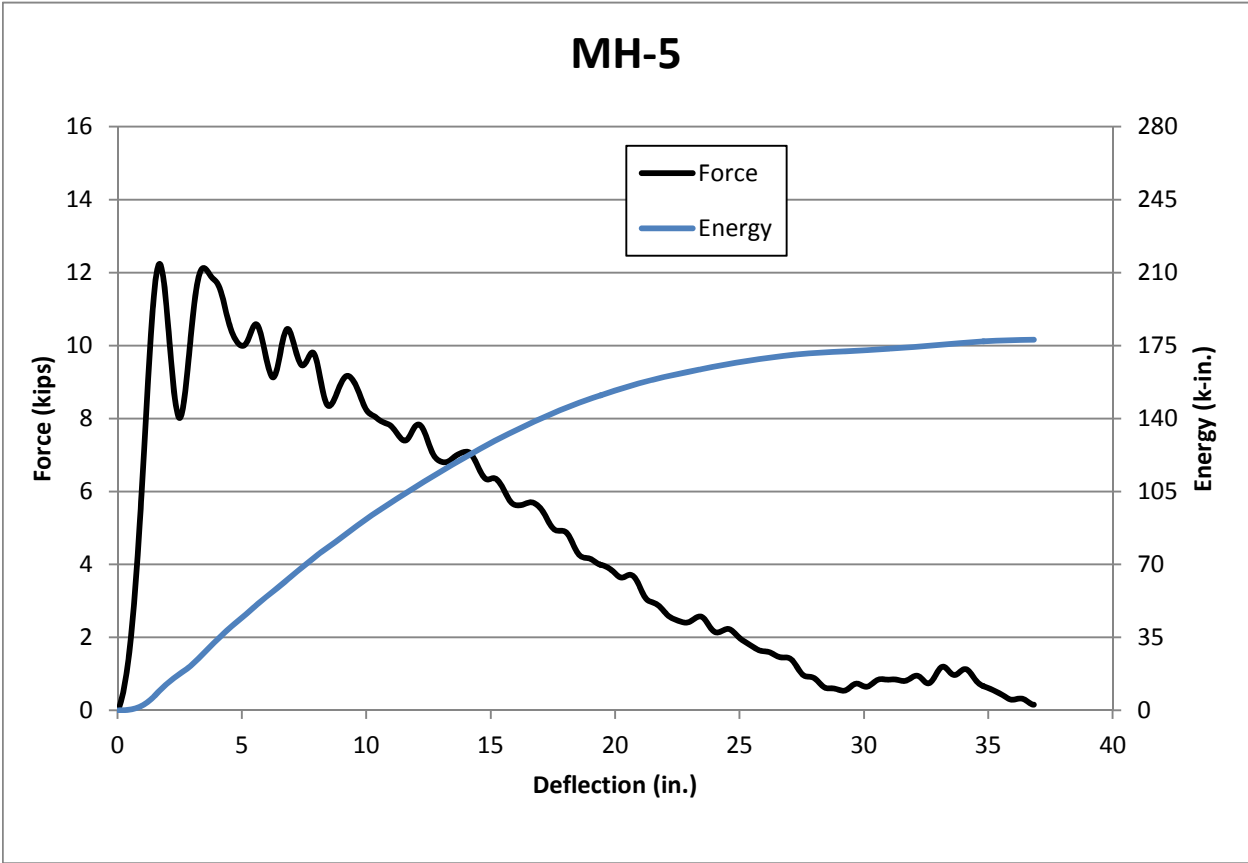
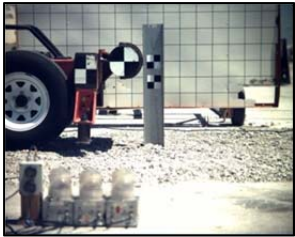


Figure 12. Force vs. Deflection and Energy vs. Deflection (DTS SLICE), Test No. MH-5





IMPACT



0.050 sec



0.100 sec



0.150 sec



0.200 sec



0.250 sec



Figure 13. Time-Sequential and Post-Impact Photographs, Test No. MH-5



### **3.2.1 Test No. MH-6**

During test no. MH-6, the bogie impacted the W6x8.5 (W152x12.6) steel post with a 36-in. (914-mm) embedment depth at a speed of 20.0 mph (32.2 km/h). As a result the post rotated through the soil. No deformation of the post occurred. The bogie vehicle overrode the post at a maximum displacement of 31.0 in. (787 mm) as determined from the accelerometer data.

Force vs. deflection and energy vs. deflection curves created from the DTS SLICE accelerometer data are shown in Figure 14. The forces quickly rose to a peak force of 13.8 kips (61.4 kN) over the first few inches of deflection. The post provided an average resistance force of around 7.9 kips (35.1 kN) through 20 in. (508 mm) of deflection. The energy absorbed by the post was 157.6 kip-in. (17.8 kJ) through 20 in. (508 mm) of deflection, and 176.6 kip-in. (20.0 kJ) through 31.0 in. (787 mm) of deflection, which corresponds to the end-of-test displacement. Time-sequential and post-impact photographs are shown in Figure 15.

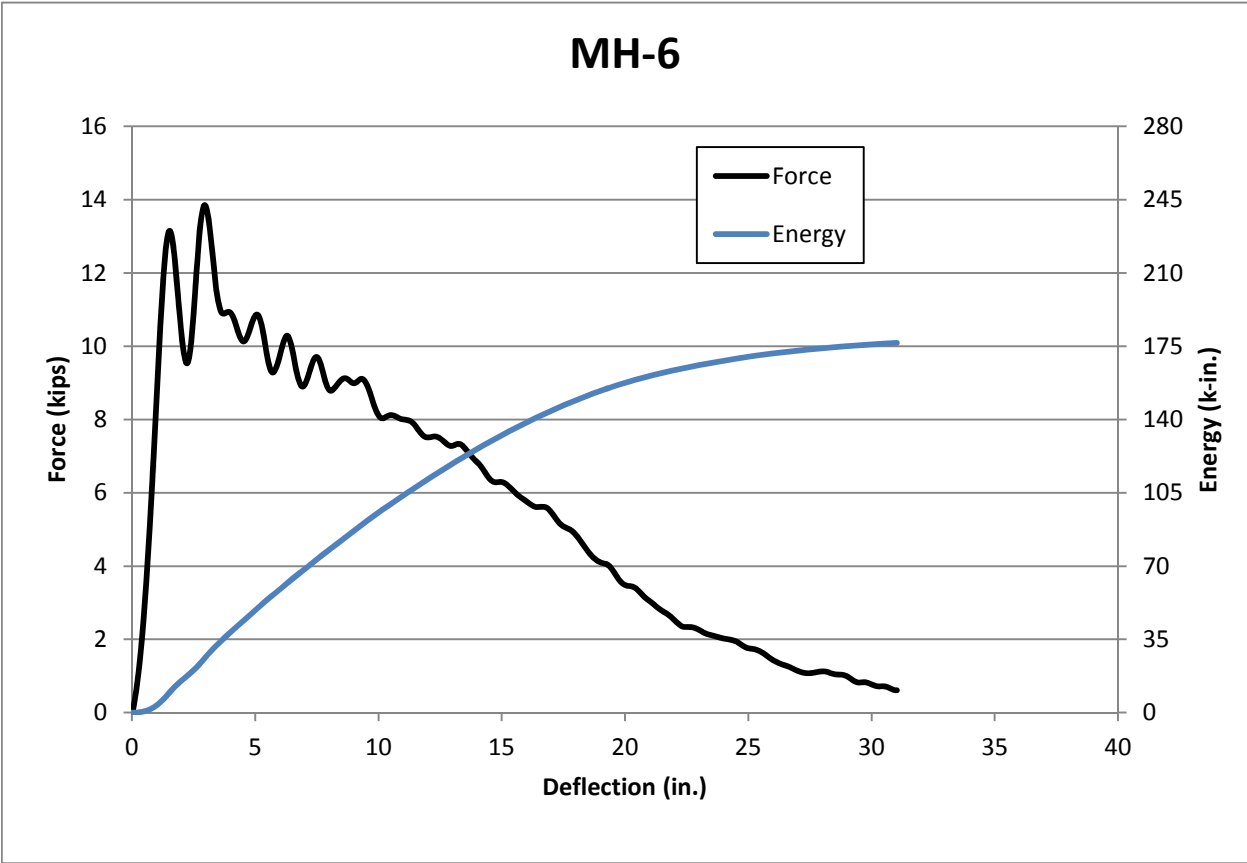


Figure 14. Force vs. Deflection and Energy vs. Deflection (DTS SLICE), Test No. MH-6



IMPACT



0.050 sec



0.100 sec



0.150 sec



0.200 sec



0.250 sec



Figure 15. Time-Sequential and Post-Impact Photographs, Test No. MH-6

### **3.2.1 Test No. MH-7**

During test no. MH-7, the bogie impacted the W6x8.5 (W152x12.6) steel post with a 36-in. (914-mm) embedment depth at a speed of 20.0 mph (32.2 km/h). As a result the post rotated through the soil. No deformation of the post occurred. The bogie vehicle overrode the post at a maximum displacement of 33.3 in. (846 mm) as determined from the accelerometer data.

Force vs. deflection and energy vs. deflection curves created from the DTS SLICE accelerometer data are shown in Figure 16. The forces quickly rose to a peak force of 10.9 kips (48.5 kN) over the first few inches of deflection. The post provided an average resistance force of around 6.4 kips (28.5 kN) through 20 in. (508 mm) of deflection. The energy absorbed by the post was 127.7 kip-in. (14.4 kJ) through 20 in. (508 mm) of deflection, and 146.7 kip-in. (16.6 kJ) through 33.3 in. (846 mm) of deflection, which corresponds to the end-of-test displacement. Time-sequential and post-impact photographs are shown in Figure 17.

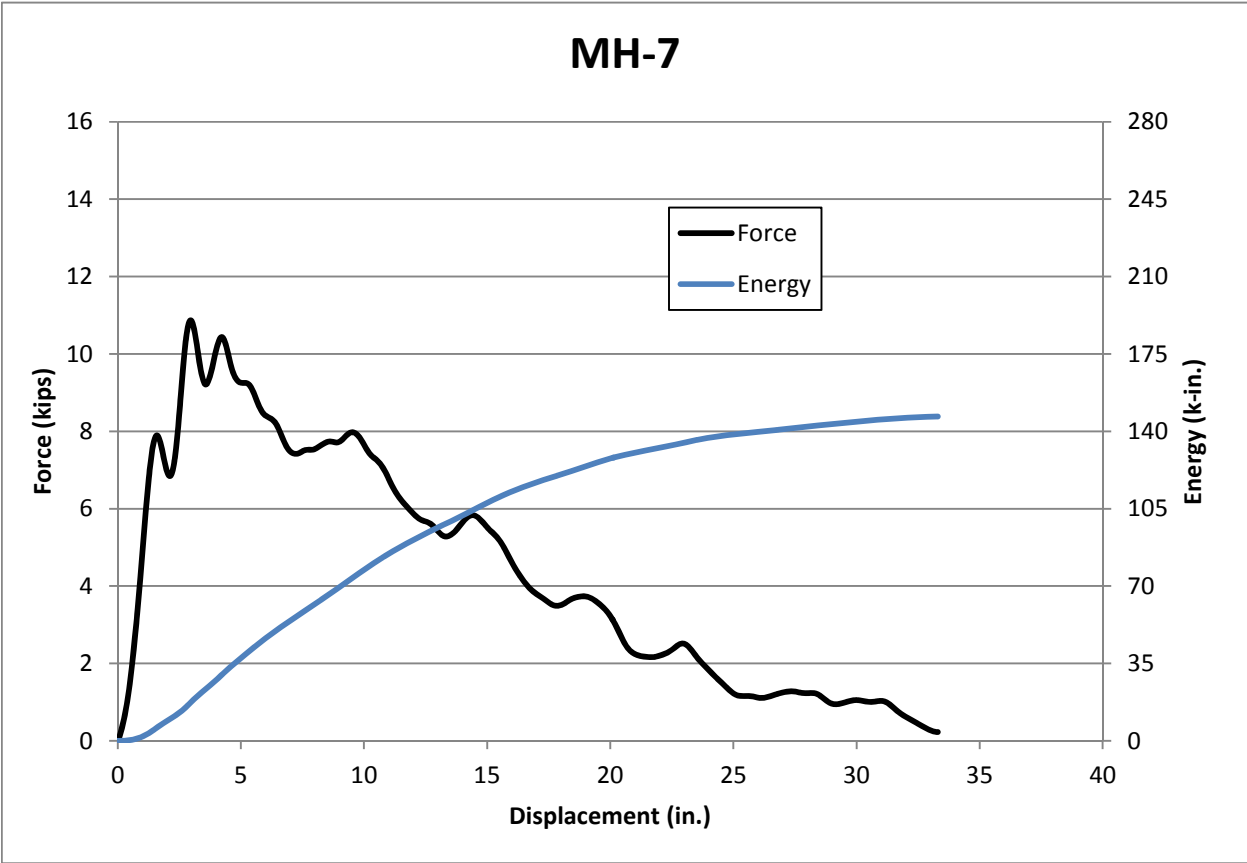


Figure 16. Force vs. Deflection and Energy vs. Deflection (DTS SLICE), Test No. MH-7





IMPACT



0.050 sec



0.100 sec



0.150 sec



0.200 sec



0.250 sec



Figure 17. Time-Sequential and Post-Impact Photographs, Test No. MH-7

### 3.2.1 Test No. MH-8

During test no. MH-8, the bogie impacted the W6x8.5 (W152x12.6) steel post with a 36-in. (914-mm) embedment depth at a speed of 20.9 mph (33.6 km/h). As a result the post rotated through the soil. No deformation of the post occurred. The bogie vehicle overrode the post at a maximum displacement of 33.8 in. (859 mm) as determined from the accelerometer data.

Force vs. deflection and energy vs. deflection curves created from the DTS SLICE accelerometer data are shown in Figure 18. The forces quickly rose to a peak force of 12.2 kips (54.3 kN) over the first few inches of deflection. The post provided an average resistance force of around 7.6 kips (33.8 kN) through 20 in. (508 mm) of deflection. The energy absorbed by the post was 151.3 kip-in. (17.1 kJ) through 20 in. (508 mm) of deflection, and 178.0 kip-in. (20.1 kJ) through 33.3 in. (859 mm) of deflection, which corresponds to the end-of-test displacement. Time-sequential and post-impact photographs are shown in Figure 19.

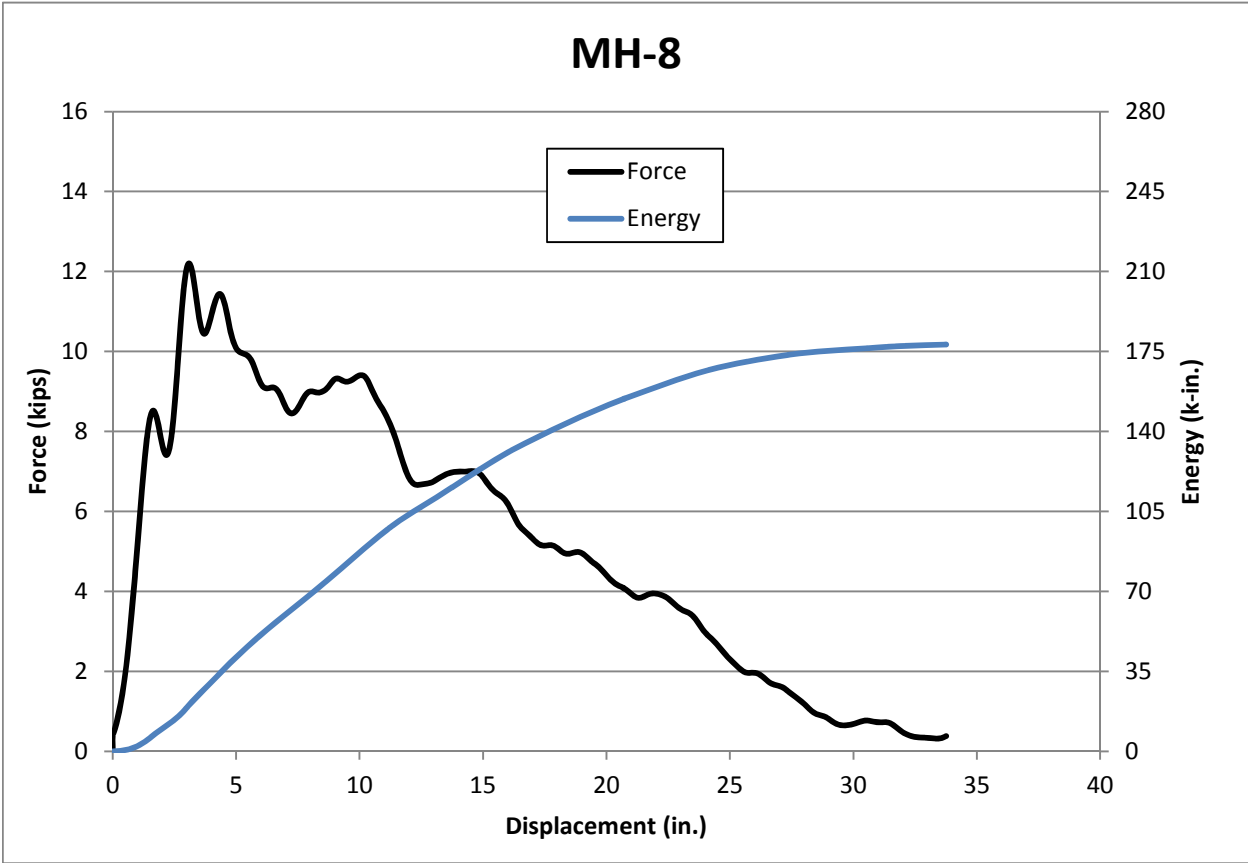
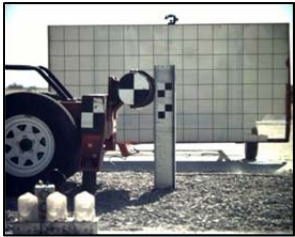


Figure 18. Force vs. Deflection and Energy vs. Deflection (DTS SLICE), Test No. MH-8





IMPACT



0.050 sec



0.100 sec



0.150 sec



0.200 sec



0.250 sec



Figure 19. Time-Sequential and Post-Impact Photographs, Test No. MH-8

### 3.3 Summary of Dynamic Testing

Eight tests were conducted on W6x8.5 (W152x12.6) steel posts at two different embedment depths and two different impact heights in order to establish the force vs. deflection and energy vs. displacement characteristics. The results from the bogie testing matrix are summarized in Table 2. The force vs. deflection comparison curves are shown in Figures 20 through 23, and the energy vs. displacement curves are shown in Figures 24 through 27.

Test nos. MH-1 and MH-4 were conducted on the W6x8.5 (W152x12.6) steel posts with a 40-in. (1,016-mm) embedment depth to give a baseline average resistance force and energy for an MGS post. These two tests, collectively referred to as “Group A,” provided very similar force vs. displacement characteristics, as shown in Figure 21. The average post-soil resistances from Group A tests were 9.5 kips (42.3 kN) and 8.9 kips (39.4 kN) through 15 in. (381 mm) and 20 in. (508 mm) of deflection, respectively. The total energy absorbed by the post was 143.7 kip-in. (16.2 kJ) and 179.0 kip-in. (20.2 kJ) through 15 in. (381 mm) and 20 in. (508 mm) of deflection, respectively. The total energy absorbed was 230.65 kip-in. (26.1 kJ) through the max deflection of 37.7 in. (596 mm).

Test nos. MH-2, MH-3, MH-5, and MH-6, collectively referred to as “Group B,” were conducted on posts with a reduced embedment depth of 36 in. (914 mm) while maintaining an impact height of 24<sup>7</sup>/<sub>8</sub> in. (733 mm). The Group B tests resulted in average forces of 8.5 kips (37.8 kN) and 7.7 kips (34.3 kN) through displacements of 15 in. (381 mm) and 20 in. (508 mm), respectively. This corresponds to 10.5 percent and 13.5 percent reductions in resistance over the same displacements when compared to the baseline tests of Group A. The total energy absorbed by the post was 127.2 kip-in. (14.4 kJ) and 155.0 kip-in. (17.5 kJ) through 15 in. (381 mm) and 20 in. (508 mm) of deflection, respectively. The total energy absorbed by the post was 183.7 kip-in. (20.8 kJ) through the max deflection of 36.0 in. (914 mm).

Test nos. MH-7 and MH-8, collectively referred to as “Group C,” utilized the reduced embedment depth of 36 in. (914 mm) in combination with an increased impact height of 28 $\frac{7}{8}$  in. (733 mm). Group C tests resulted in average forces of 7.8 kips (34.7 kN) and 7.0 kips (31.1 kN) through displacements of 15 in. (381 mm) and 20 in. (508 mm), respectively. The total energy absorbed by the post was 116.0 kip-in. (13.1 kJ) and 139.5 kip-in. (15.8 kJ) through 15 in. (381 mm) and 20 in. (508 mm) of deflection, respectively. The total energy absorbed by the post was 162.4 kip-in. (18.3 kJ) through the max deflection of 33.6 in. (853 mm). These values correlate to 17.9 percent and 21.3 percent reductions in forces when compared to the Group A results. Thus, the Group C tests had even lower resistance and energy absorption than the Group B tests.

Reductions in forces and energy absorption were expected for both Group B and Group C tests as both reduced post embedment depths and increased impact heights have been shown to result in lower resistance. In a 2012 report, Jowza [6] provided the following equation for calculating the change in average resistance force due to changes in the impact height and the post embedment depth:

$$F_2 = F_1 \left( \frac{MA_1}{MA_2} \right) \left( \frac{Emb_2}{Emb_1} \right)^2 \quad (\text{Eq-1})$$

Where:

F = the average resistance force

MA = length of the moment arm in the post (defined as the distance from the impact point to the point of rotation in the post)

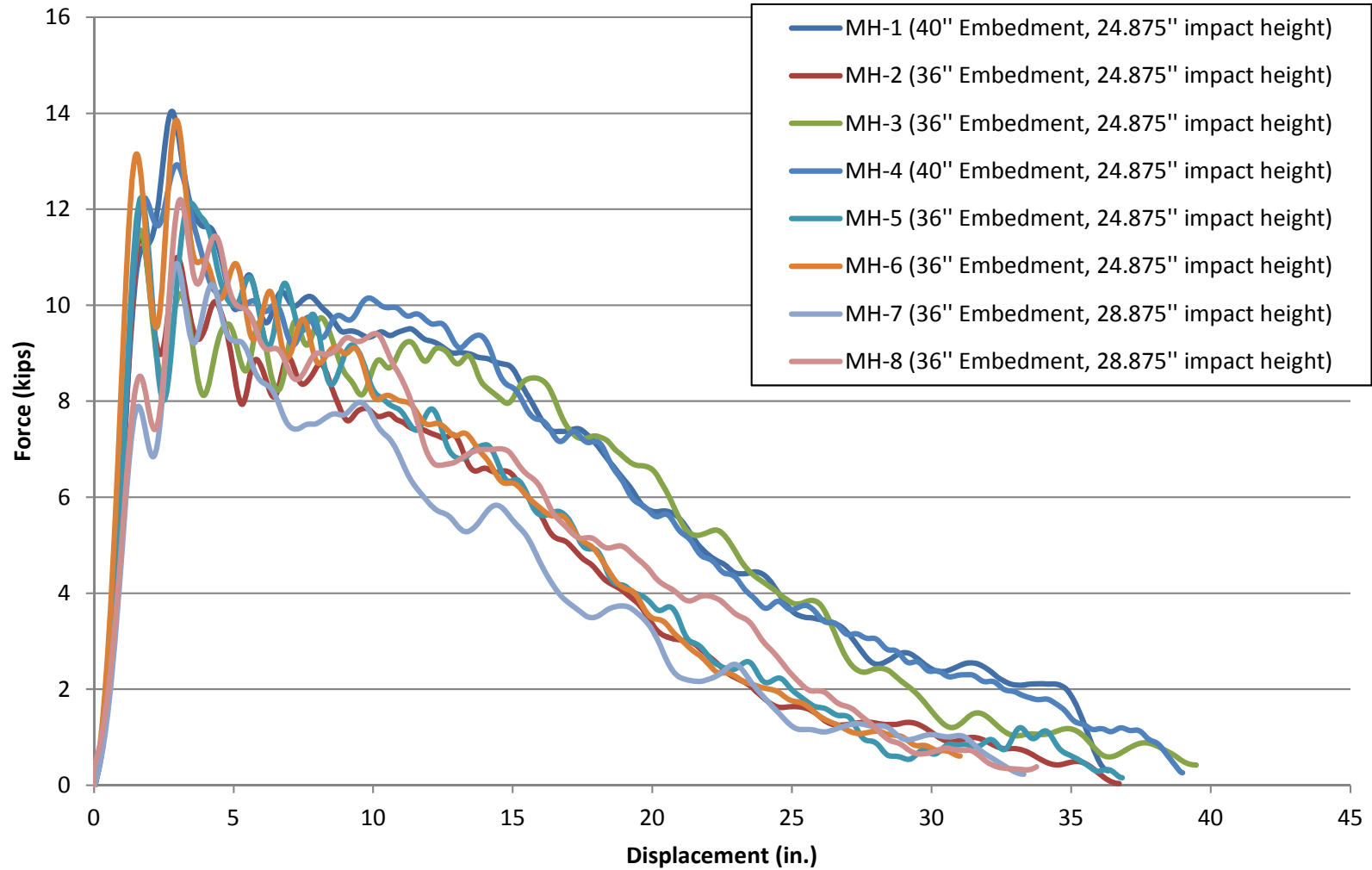
Emb = post embedment depth

Table 2. Dynamic Testing Results

36

Test No.	Impact Speed mph (km/h)	Peak Force kips (kN)	Average Force kips (kN)			Max Deflection in. (mm)	Energy kip-in. (kJ)			Failure Type
			at 10"	at 15"	at 20"		at 15"	at 20"	Total	
<b>Group A: 40 in. (1,016 mm) Embedment, 24<math>\frac{1}{8}</math> in. (632 mm) load height</b>										
MH-1	20.8 (33.5)	14.0 (62.3)	9.8 (43.6)	9.5 (42.3)	8.8 (39.1)	36.3 (922)	143.9 (16.3)	179.4 (20.3)	230.6 (26.1)	Rotation in Soil and Yielding
MH-4	20.5 (33.0)	12.9 (57.4)	9.6 (42.7)	9.5 (42.3)	8.9 (39.6)	39.0 (991)	143.4 (16.2)	178.5 (20.2)	230.7 (26.1)	Rotation in Soil and Yielding
<b>Averages</b>		13.5 (59.8)	9.7 (43.1)	9.5 (42.3)	8.9 (39.4)	37.7 (956)	143.7 (16.2)	179.0 (20.2)	230.7 (26.1)	
<b>Group B: 36 in. (914 mm) Embedment, 24<math>\frac{1}{8}</math> in. (632 mm) load height</b>										
MH-2	20.8 (33.5)	11.5 (51.2)	8.3 (36.9)	7.9 (35.1)	7.0 (31.1)	36.7 (932)	118.8 (13.4)	142.8 (16.1)	165.9 (18.7)	Rotation in Soil
MH-3	21.7 (33.5)	11.6 (51.6)	8.5 (37.8)	8.6 (38.3)	8.3 (36.9)	39.5 (1,003)	129.1 (14.6)	166.3 (18.8)	214.3 (24.2)	Rotation in Soil
MH-5	19.9 (32.0)	12.2 (54.3)	9.2 (40.9)	8.5 (37.8)	7.7 (34.3)	36.8 (935)	128.3 (14.5)	153.4 (17.3)	177.8 (20.1)	Rotation in Soil
MH-6	20.0 (32.2)	13.8 (61.4)	9.5 (42.3)	8.8 (39.1)	7.9 (35.1)	31.0 (787)	132.6 (15.0)	157.6 (17.8)	176.6 (20.0)	Rotation in Soil
<b>Averages</b>		12.3 (54.7)	8.9 (39.6)	8.5 (37.8)	7.7 (34.3)	36.0 (914)	127.2 (14.4)	155.0 (17.5)	183.7 (20.8)	
<b>Group C: 36 in. (914 mm) Embedment, 28<math>\frac{1}{8}</math> in. (733 mm) load height</b>										
MH-7	20.0 (32.2)	10.9 (48.5)	7.7 (34.3)	7.2 (32.0)	6.4 (28.5)	33.3 (846)	107.6 (12.2)	127.7 (14.4)	146.7 (16.6)	Rotation in Soil
MH-8	20.8 (33.5)	12.2 (54.3)	8.7 (38.7)	8.3 (36.9)	7.6 (33.8)	33.8 (859)	124.4 (14.1)	151.3 (17.1)	178.0 (20.1)	Rotation in Soil
<b>Averages</b>		11.6 (51.4)	8.2 (36.5)	7.8 (34.7)	7.0 (31.1)	33.6 (853)	116.0 (13.1)	139.5 (15.8)	162.4 (18.3)	

## W6x8.5 (W152x12.6) Steel Posts



37

Figure 20. Force vs. Deflection Comparison, Test Nos. MH-1 through MH-8

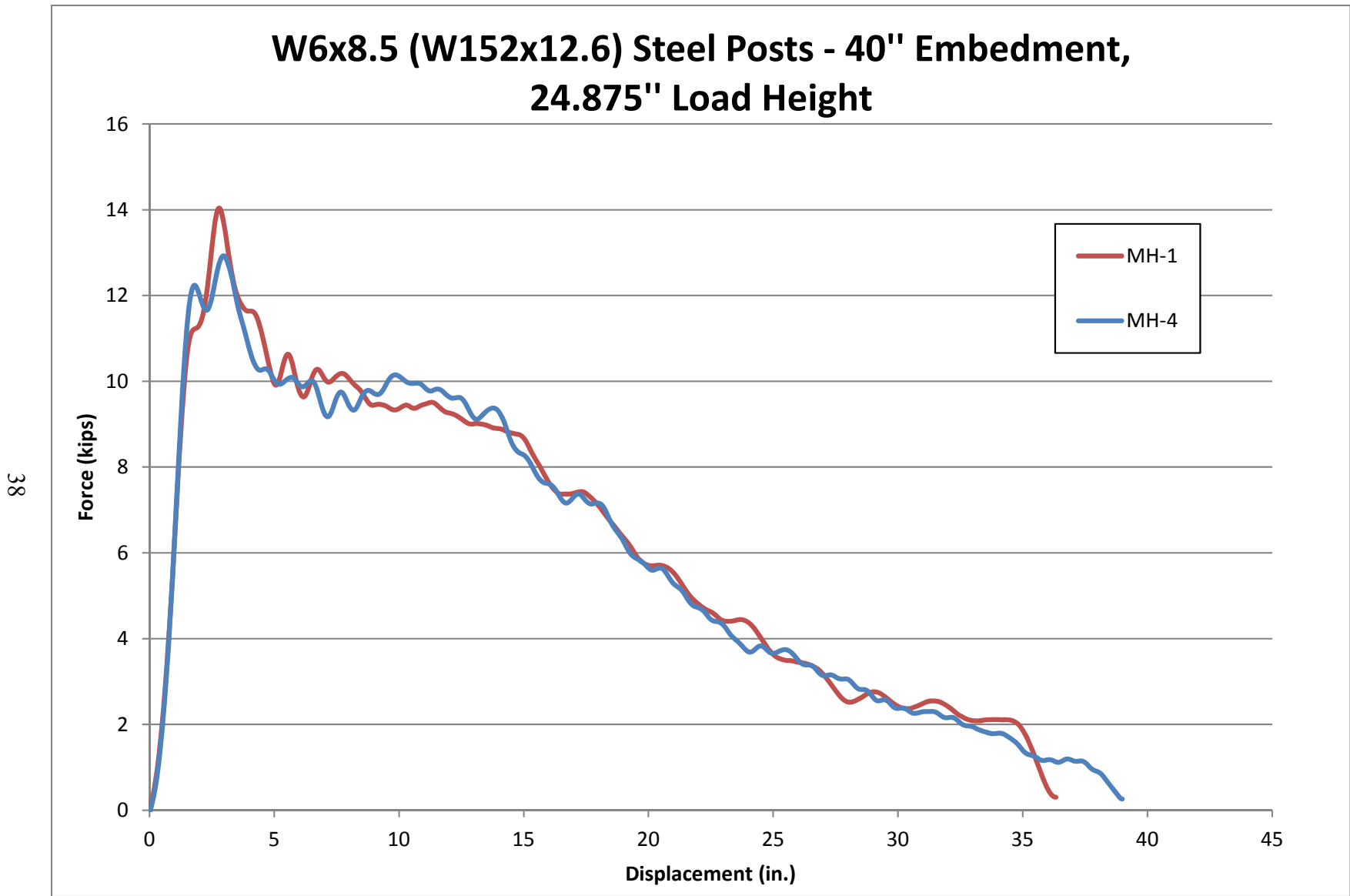


Figure 21. Force vs. Deflection Plots, 40 in. Embedment and 24.875 in. Load Height

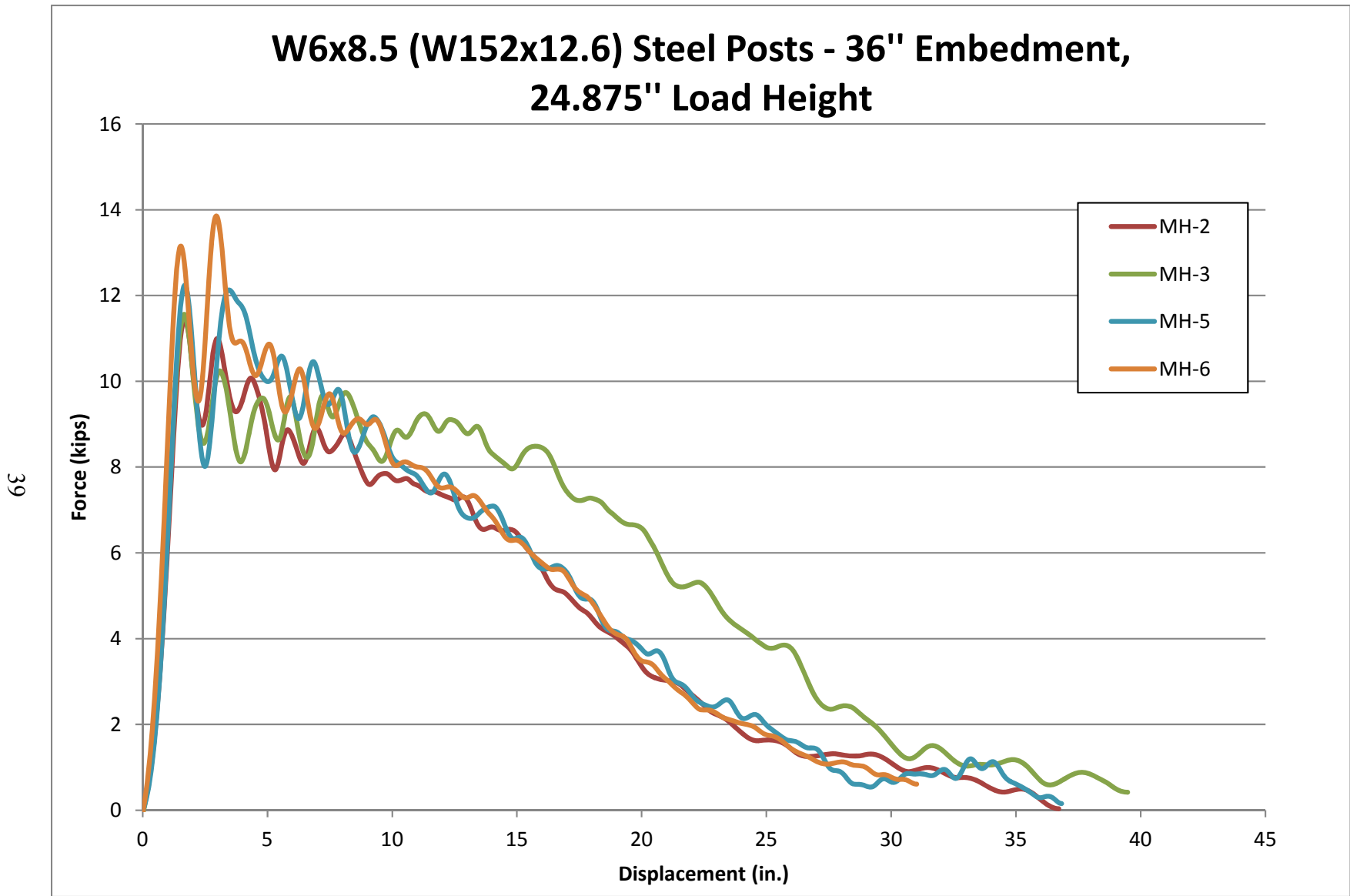


Figure 22. Force vs. Deflection Plots, 36 in. Embedment and 24.875 in. Load Height

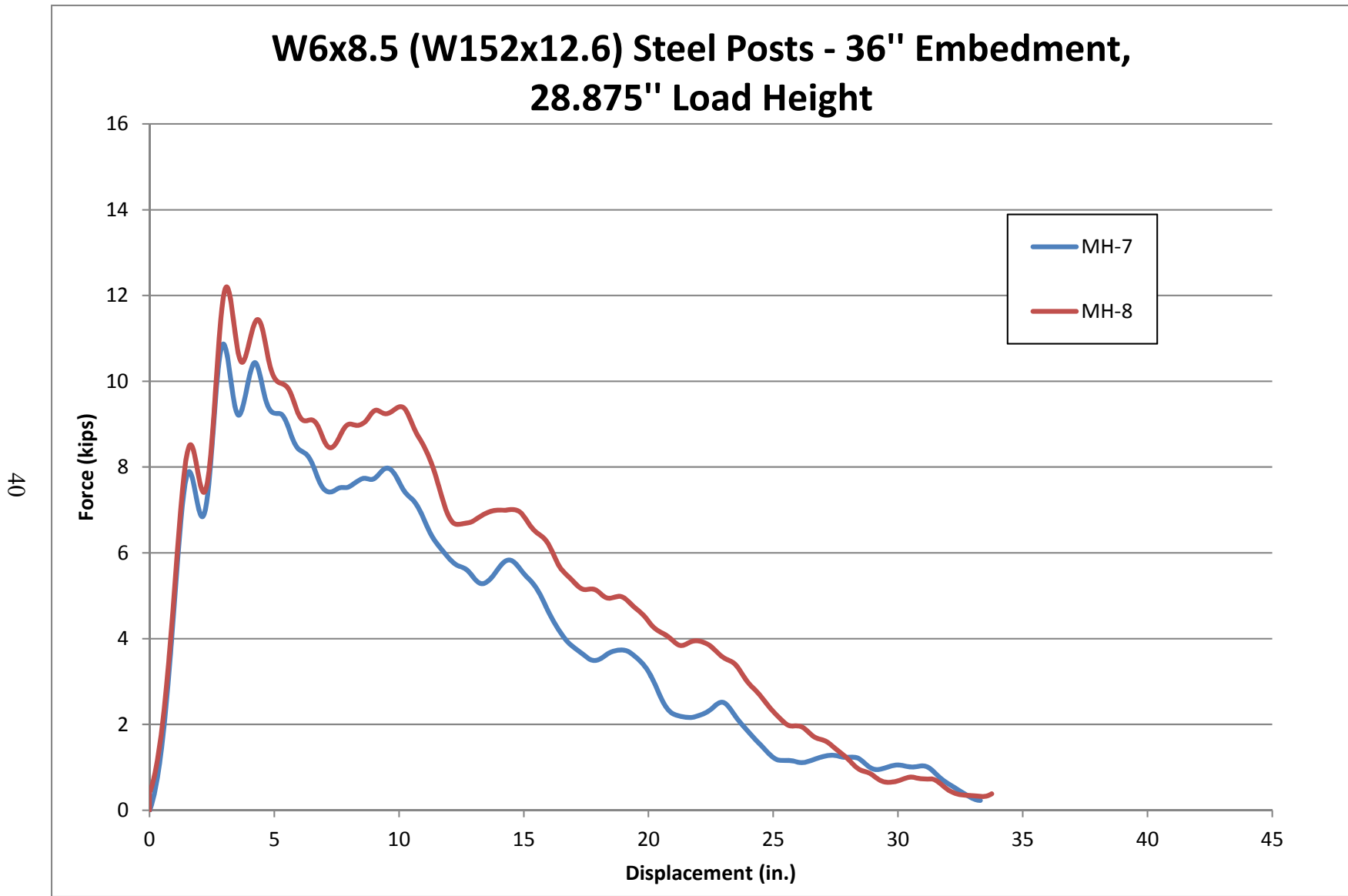


Figure 23. Force vs. Deflection Comparison, Test Nos. MH-1 through MH-8



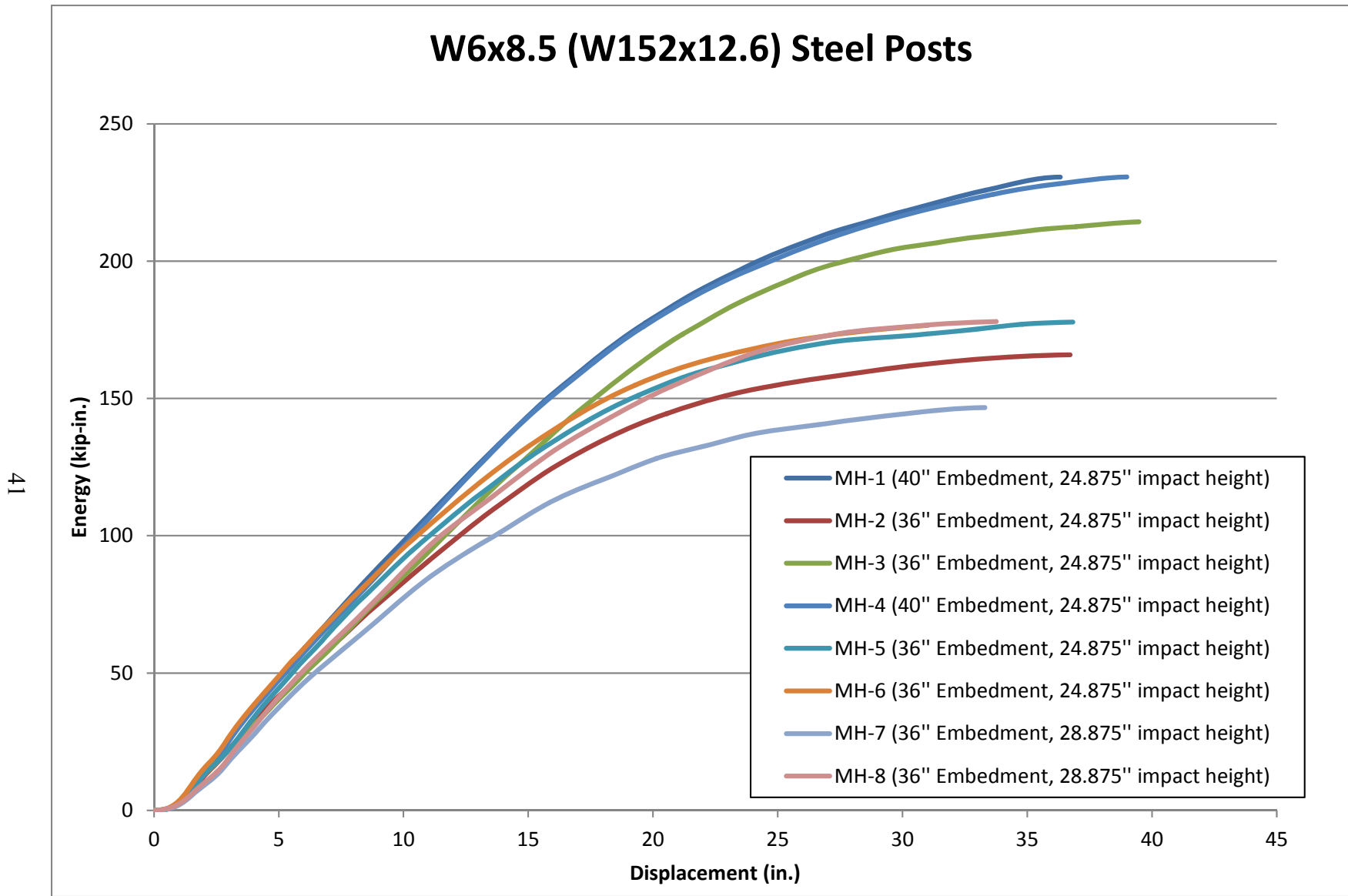


Figure 24. Energy vs. Displacement Plots, 36 in. Embedment and 28 7/8 in. Load Height

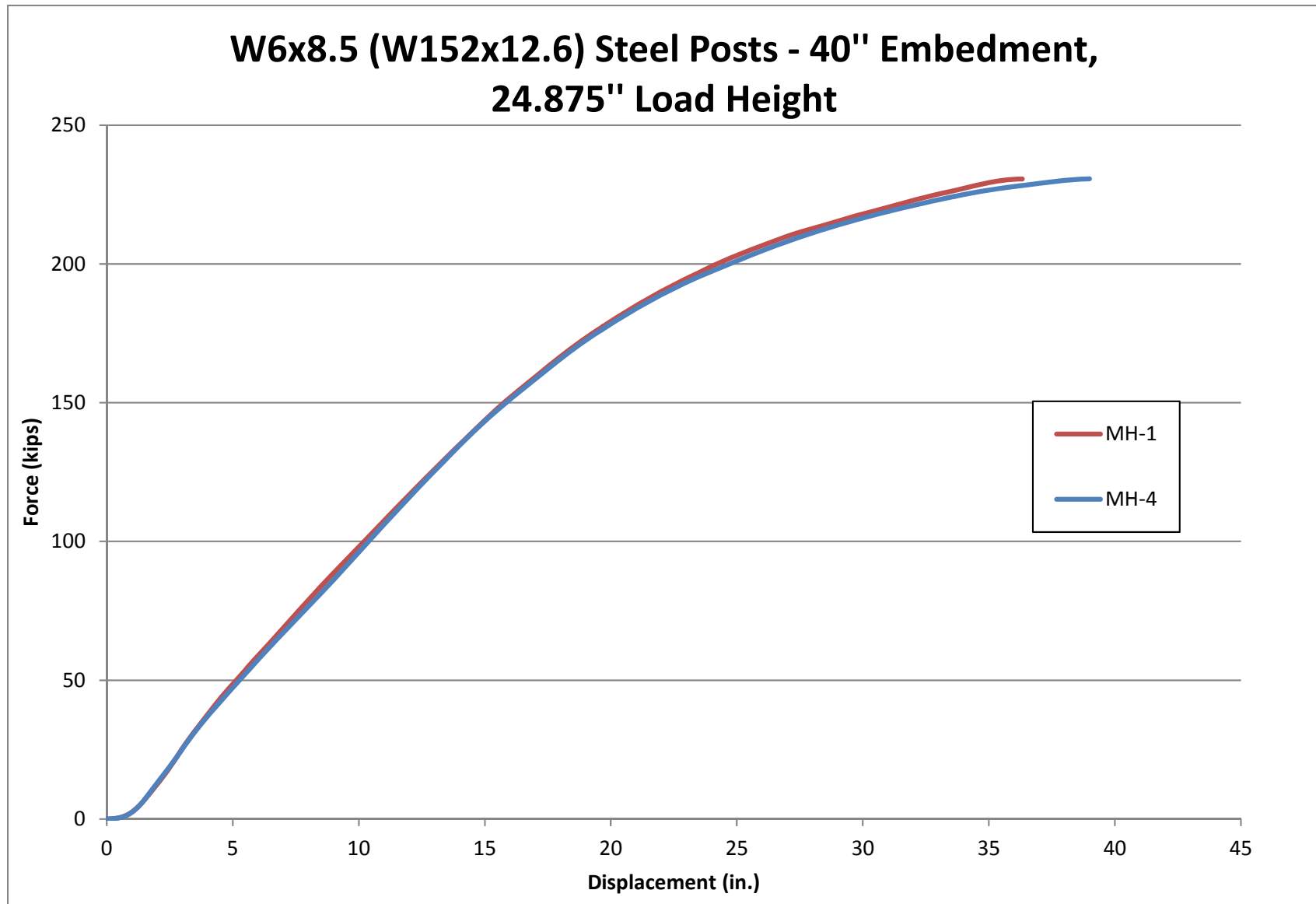
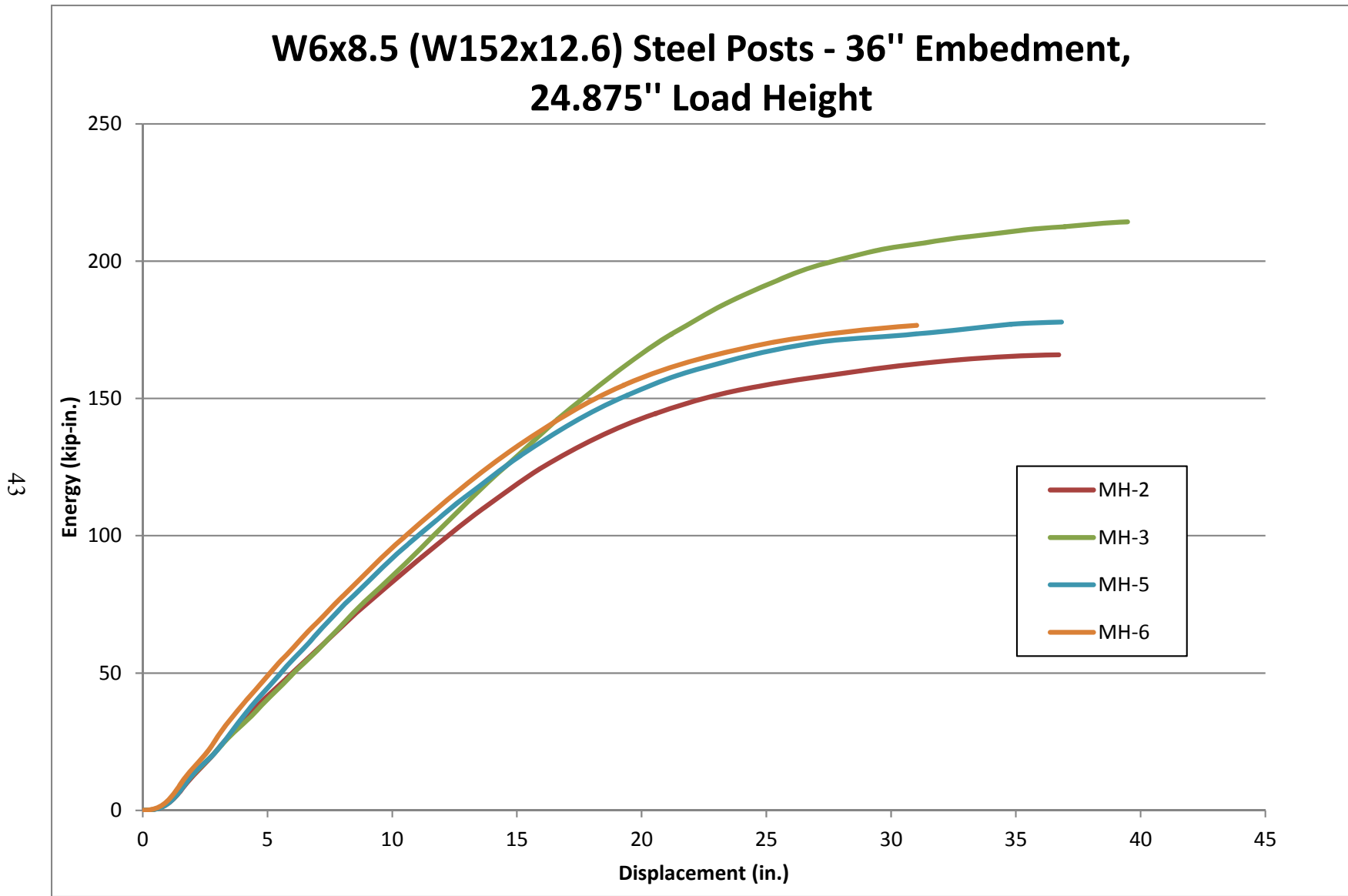


Figure 25. Energy vs. Displacement Plots, 40 in. Embedment and 24 $\frac{7}{8}$  in. Load Height



43

Figure 26. Energy vs. Displacement Plots, 36 in. Embedment and 24.875 in. Load Height

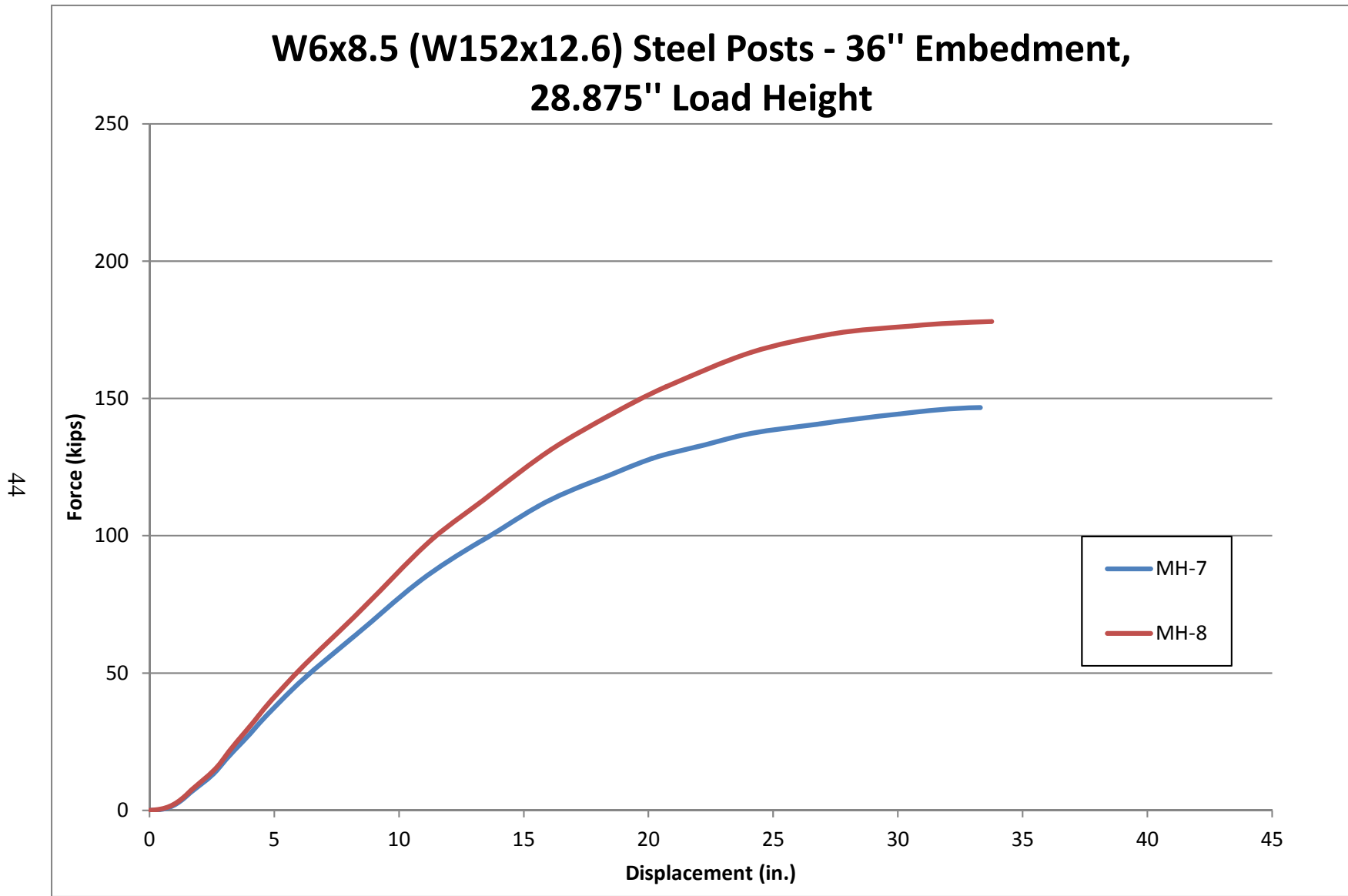


Figure 27. Energy vs. Displacement Plots, 36 in. Embedment and 28.875 in. Load Height

Equation-1 was utilized to predict the average resistance force under three different cases: (1) using Group A data to predict Group B results; (2) using Group B results to predict Group C results; and (3) using Group A results to predict Group C results. These predicted average resistance forces were then compared to the actual bogie test results to gauge the accuracy of the equation. The results of these calculations are shown in Table 3.

Although the values for embedment depth are straightforward, the value for the moment arm distance is dependent upon the location of the rotation point. Depending on the study, assumptions have been made placing the rotation point as high as ground line and as low as  $\frac{2}{3}$  of the embedment depth [6-7]. Therefore, the predicted average forces were calculated utilizing both of these extremes to bracket the analysis results. Overall, assuming a rotation point at  $\frac{2}{3}$  of the embedment depth provided more accurate results as the predicted average forces were always within 5 percent of the actual test results.

Table 3. Comparison of Predicted Results to Actual Test Results

Group Calculation Case	Tested Average Forces		Moment Arm = Ground Line to Impact Pt.		Moment Arm = $\frac{2}{3}$ Emb. to Impact Pt.	
	F <sub>1</sub> (kips)	F <sub>2</sub> (kips)	Estimated F <sub>2</sub> (kips)	Predicted to Tested Ratio (Est. F <sub>2</sub> / F <sub>2</sub> )	Estimated F <sub>2</sub> (kips)	Predicted to Tested Ratio (Est. F <sub>2</sub> / F <sub>2</sub> )
Forces Calculated at 15 in. of deflection						
A - B	9.5	8.5	7.70	0.91	8.11	0.95
B - C	8.5	7.8	7.32	0.94	7.86	1.01
A - C	9.5	7.8	6.63	0.85	7.50	0.96
Forces Calculated at 20 in. of deflection						
A - B	8.9	7.7	7.21	0.94	7.60	0.99
B - C	7.7	7.0	6.63	0.95	7.12	1.02
A - C	8.9	7.0	6.21	0.89	7.03	1.00

A = 40 in. (1,016 mm) embedment and  $24\frac{7}{8}$  in. (632 mm) load height  
B = 36 in. (914 mm) embedment and  $24\frac{7}{8}$  in. (632 mm) load height  
C = 36 in. (914 mm) embedment and  $28\frac{7}{8}$  in. (733 mm) load height

In general, the predicted force values were relatively accurate but tended to be lower than the actual test results. This can be explained by the fact that the Group A posts had plastically deformed during the tests. Thus, some of the impact energy was absorbed by the post yielding. Equation-1 predicts the average post-soil resistance assumes only soil deformation. Therefore, using Group A results to predict the resistance for other posts would result in underestimating the true resistances. However, this underestimation proved to be minor as the analysis still provided predicted average forces within 15 percent of the actual test data for all cases.

#### 4 SUMMARY AND CONCLUSIONS

The objective of this research study was to determine the force vs. deflection characteristics for MGS steel posts with reduced embedment depths and increased load heights. Eight dynamic component tests were conducted on 72-in. (1,829-mm) long W6x8.5 (W152x12.6) posts. Group A consisted of two tests (test nos. MH-1 and MH-4) and were conducted with an embedment depth of 40 in. (1,016 mm) with an impact height of 24<sup>7</sup>/<sub>8</sub> in. (632 mm). These conditions matched those of standard MGS installations and provided the baseline for which to compare the other results. Group B consisted of four tests (test nos. MH-2, MH-3, MH-5, and MH-6) and were conducted on posts with an embedment depth of 36 in. (914 mm) with an impact height of 24<sup>7</sup>/<sub>8</sub> in. (632 mm). Group C consisted of two tests (test nos. MH-7 and MH-8) and were conducted on posts with an embedment depth of 36 in. (914 mm) with an impact height of 28<sup>7</sup>/<sub>8</sub> in. (733 mm). All eight tests were conducted with a target impact speed of 20 mph (32.2 km/h).

The two W6x8.5 (W152x12.6) posts with a 40-in. (1,016-mm) embedment depth yielded during testing. Both posts were from the Group A tests and developed plastic hinges approximately 10 in. (254 mm) below ground line. None of the posts with the 36-in. (914-mm) embedment depths yielded. Even the Group C posts with the increased load height remained undamaged.

As expected, the Group B posts with a reduced embedment depth resulted in lower post-soil interaction forces. In fact, the average resistance force was decreased approximately 12 percent as compared to the average forces recorded during the baseline, or Group A tests. The resistance was further reduced during the Group C tests when the load height was increased. The Group C tests showed average resistance forces approximately 20 percent lower than those of Group A.



The test results were also analyzed using Equation-1 which is used to predict the average resistance force of a post rotating through soil due to a change in embedment depth or load height. This analysis concluded that Equation-1 can be used to predict average resistance forces with considerable accuracy. The predicted average forces were all within 15 percent of the actual test results. However, the accuracy of Equation-1 was directly related to the location of the assumed post rotation point. The accuracy was increased to within 5 percent when the rotation point of the post was assumed to be  $\frac{2}{3}$  of the embedment depth as opposed to near ground line. Thus, the true rotation point for MGS posts installed on flat ground is most likely within the bottom half of the embedment depth.

## 5 REFERENCES

1. *Manual for Assessing Safety Hardware (MASH)*, American Association of State Highway and Transportation Officials (AASHTO), Washington, D.C., 2009.
2. Polivka, K.A., Faller, R.K., Sicking, D.L., Rohde, J.R., Bielenberg, B.W., and Reid, J.D., *Performance Evaluation of the Midwest Guardrail System-Update to NCHRP 350 Test No. 3-11 with 28" C.G. Height (2214MG-2)*, Final Report to National Cooperative Highway Research Program, MwRSF Research Report No. TRP-03-171-06, Midwest Roadside Safety Facility, University of Nebraska-Lincoln, Lincoln, Nebraska, October 11, 2006.
3. Polivka, K.A., Faller, R.K., Sicking, D.L., Rohde, J.R., Bielenberg, B.W., and Reid, J.D., *Performance Evaluation of the Midwest Guardrail System-Update to NCHRP 350 Test No. 3-10 (2214MG-3)*, Final Report to National Cooperative Highway Research Program, MwRSF Research Report No. TRP-03-172-06, Midwest Roadside Safety Facility, University of Nebraska-Lincoln, Lincoln, Nebraska, October 11, 2006.
4. Griffith, M.S., FHWA MASH approval letter B-212 of Midwest Guardrail System (MGS), To K.A. Lechtenberg, Midwest Roadside Safety Facility, Lincoln, NE, December 18, 2010.
5. Society of Automotive Engineers (SAE), *Instrumentation for Impact Test – Part 1 – Electronic Instrumentation*, SAE J211/1 MAR95, New York City, NY, July, 2007.
6. Jowza, E.R., Faller, R.K., Rosenbaugh, S.K., Sicking, D.L., Reid, J.D., *Safety Investigation and Guidance for Retrofitting Existing Approach Guardrail Transitions*, Final Report to the Wisconsin Department of Transportation, Transportation Research Report No. TRP-03-266-12, Project Code: TPF-5(193) Supp. #26, Midwest Roadside Safety Facility, University of Nebraska-Lincoln, Lincoln, Nebraska, August 21, 2012.
7. Coon, B., Dynamic Impact Testing and Simulation of Guardrail Posts Embedded in Soil, Thesis, University of Nebraska – Lincoln, December 1999.

## **6 APPENDICES**

## **Appendix A. Material Certifications**

**GREGORY HIGHWAY PRODUCTS, INC.**  
**4100 13th St. P.O. Box 80508**  
**Canton, Ohio 44708**

**Customer:** MIDWEST MACHINERY & SUPPLY CO.  
 2200 Y STREET  
 LINCOLN, NE, 68501

Test Report  
 B.O.L. # 5239AA-1  
 Customer P.O.: 2551  
 Shipped to: MIDWEST MACHINERY & SUPPLY CO.  
 Project: STOCK  
 GHP Order No. 5239AA

DATE SHIPPED: 02/29/12

HT # code	C.	Mn.	P.	S.	Si.	Tensile	Yield	Elong.	Quantity	Class	Type	Description
L81665	0.1	0.8	0.01	0.025	0.19	63000	53300	20	200	2	2	6IN WF AT 8.5 X 6FT 0IN GR POST
L83827	0.09	0.94	0.013	0.031	0.23	70400	56300	24	200	2	2	6IN WF AT 8.5 X 6FT 0IN GR POST
L83786	0.09	0.85	0.011	0.038	0.23	66500	52300	20	200	2	2	6IN WF AT 8.5 X 6FT 0IN GR POST
L83766	0.09	0.88	0.011	0.036	0.19	67200	53300	21	200	2	2	6IN WF AT 8.5 X 6FT 0IN GR POST
L81670	0.09	0.92	0.014	0.028	0.2	62000	47400	21	50	2	2	6IN WF AT 8.5 X 6FT 0IN GR POST

52

Bolts comply with ASTM A-307 specifications and are galvanized in accordance with ASTM A-153, unless otherwise stated.  
 Nuts comply with ASTM A-563 specifications and are galvanized in accordance with ASTM A-153, unless otherwise stated.  
 All other galvanized material conforms with ASTM-123 & ASTM-653  
 All steel used in the manufacture is of Domestic Origin, "Made and Melted in the United States"  
 All Guardrail and Terminal Sections meets AASHTO M-180, All structural steel meets AASHTO M-183 & M270  
 All Bolts and Nuts are of Domestic Origin  
 All material fabricated in accordance with Nebraska Department of Transportation  
 All controlled oxidized/corrosion resistant Guardrail and terminal sections meet ASTM A606, Type 4.

By: *Andrew Artar*  
 Andrew Artar  
 Vice President of Sales & Marketing  
 Gregory Highway Products, Inc.

STATE OF OHIO: COUNTY OF STARK  
 Sworn to and subscribed before me, a Notary Public, by  
 Andrew Artar this 1st day of March 2012  
 James P. Dehnke  
 Notary Public, State of Ohio  
 My Commission Expires 10-19-2014




Figure A-1. Post Material Certification, Test Nos. MH-1 through MH-8

## **Appendix B. Soil Batch Sieve Analysis**

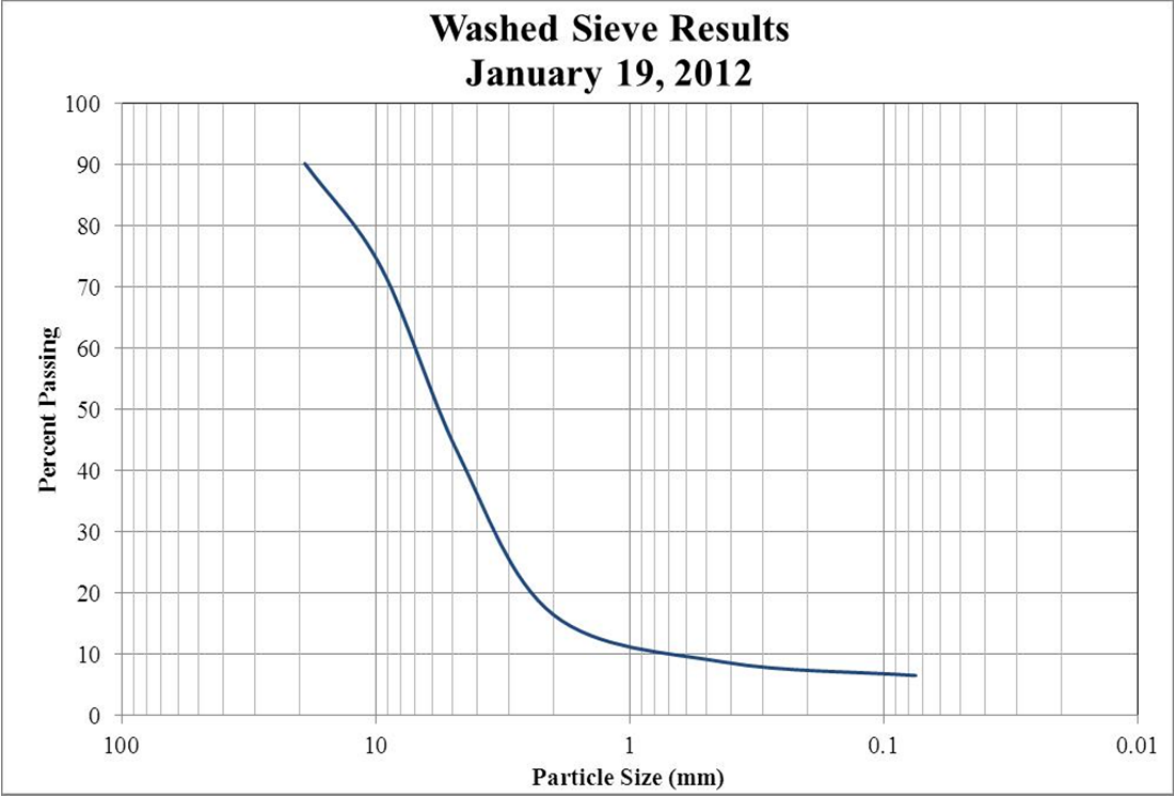


Figure B-1. Soil Gradation for Test Nos. MH-1 through MH-8

### **Appendix C. Bogie Test Results**

The results of the recorded data from each accelerometer for every dynamic bogie test are provided in the summary sheets found in this appendix. Summary sheets include acceleration, velocity, and deflection vs. time plots as well as force vs. deflection and energy vs. deflection plots.



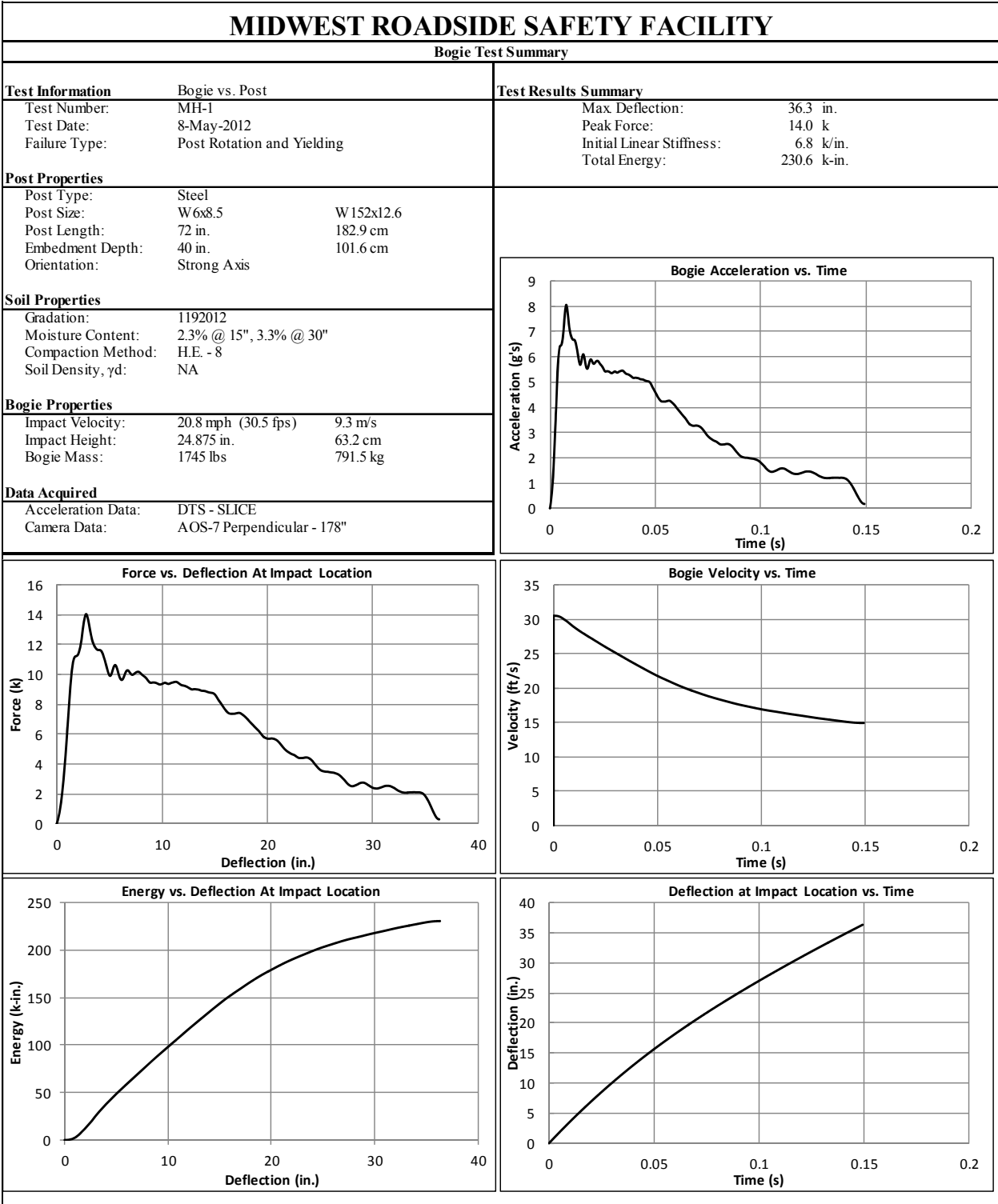


Figure C-1. Test No. MH-1 Results (DTS SLICE)

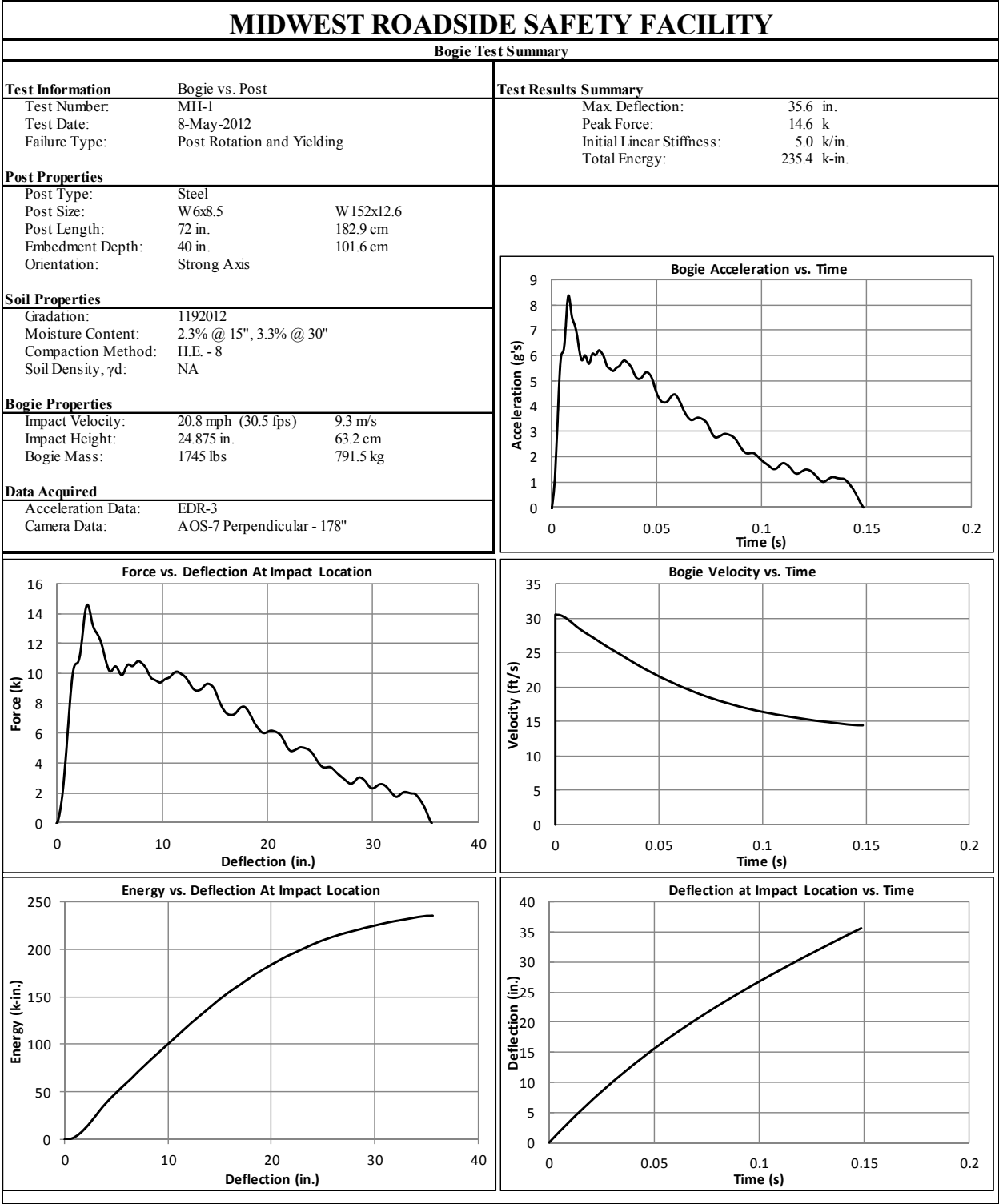


Figure C-2. Test No. MH-1 Results (EDR-3)

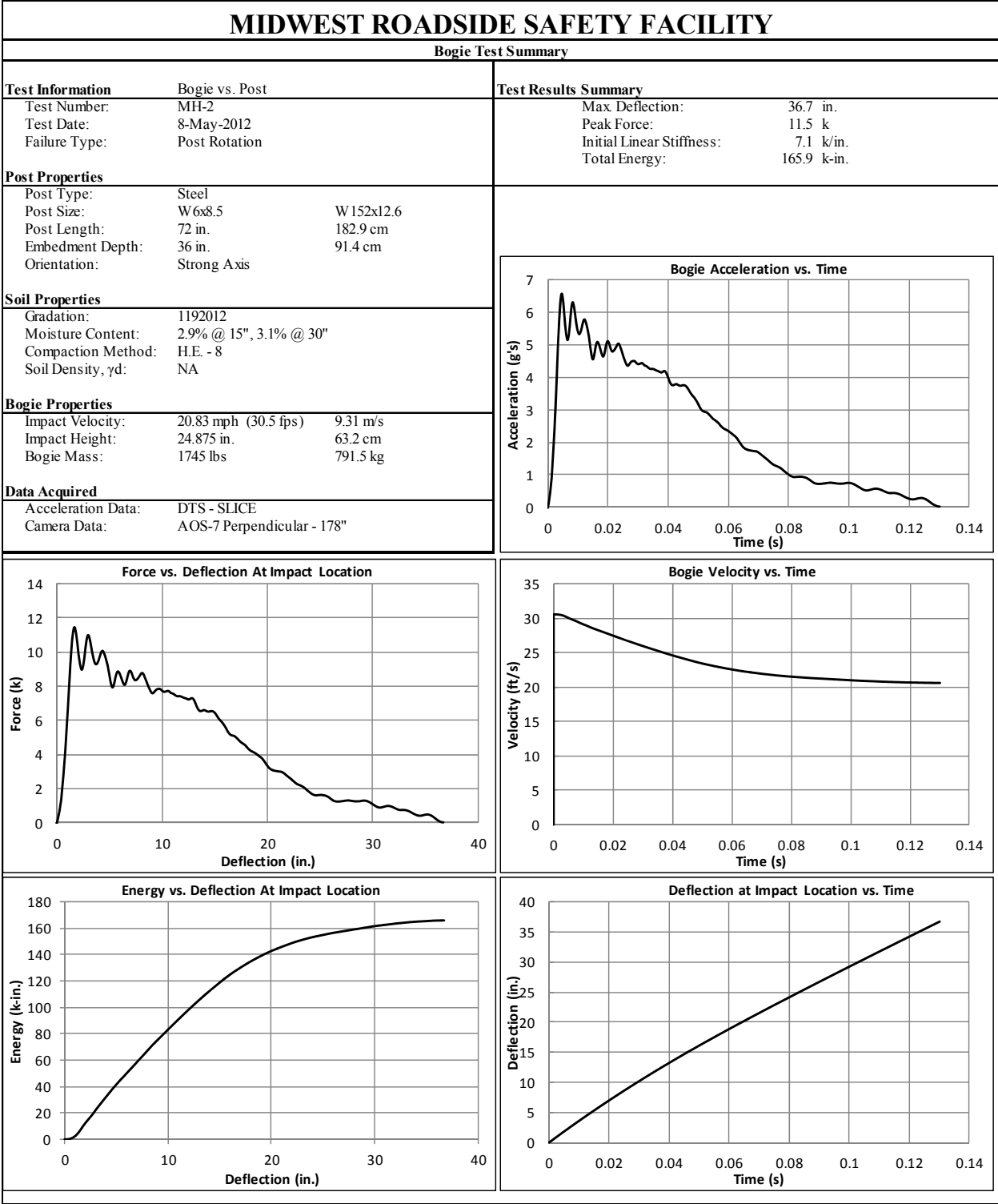


Figure C-3. Test No. MH-2 Results (DTS SLICE)

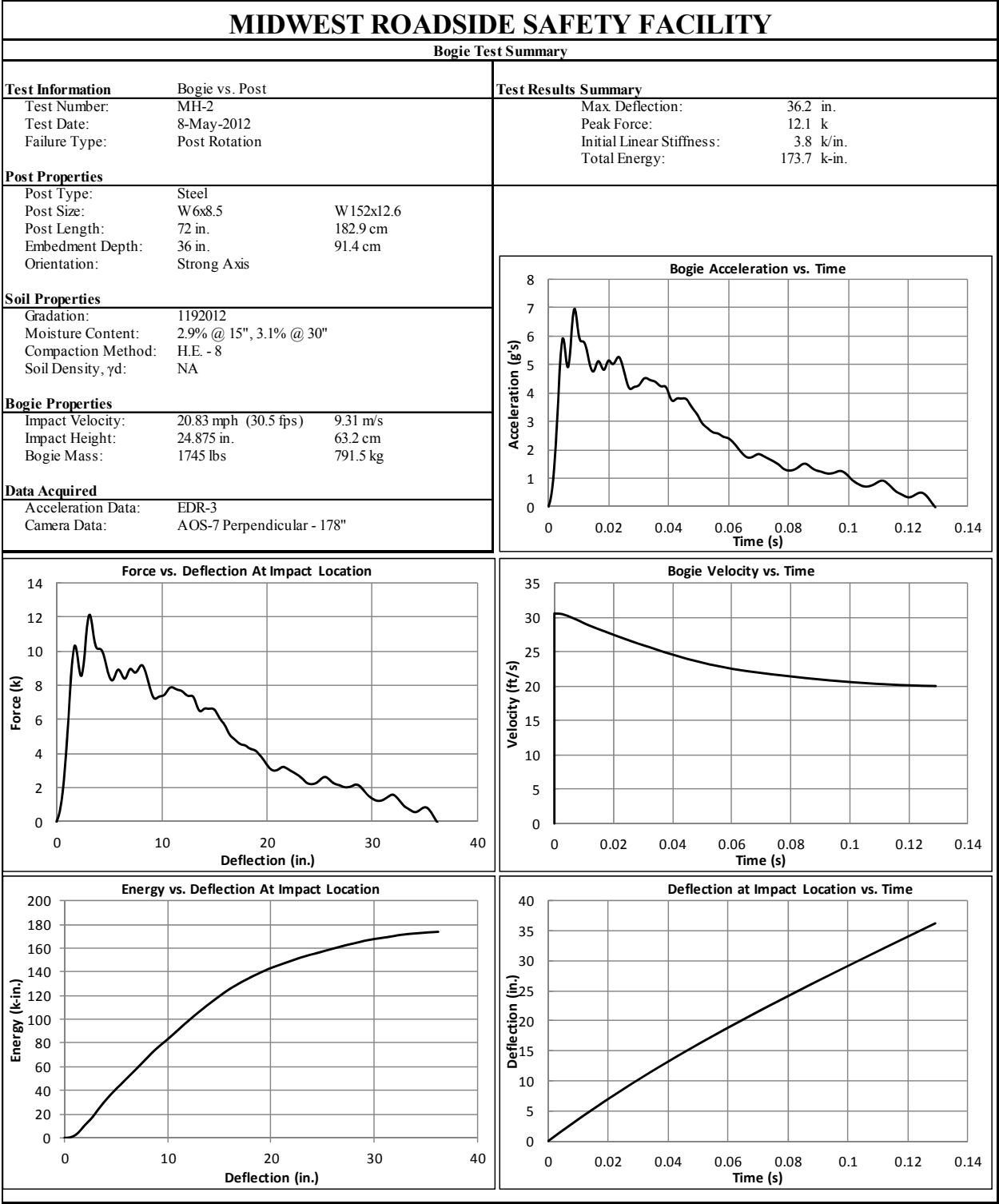


Figure C-4. Test No. MH-2 Results (EDR-3)

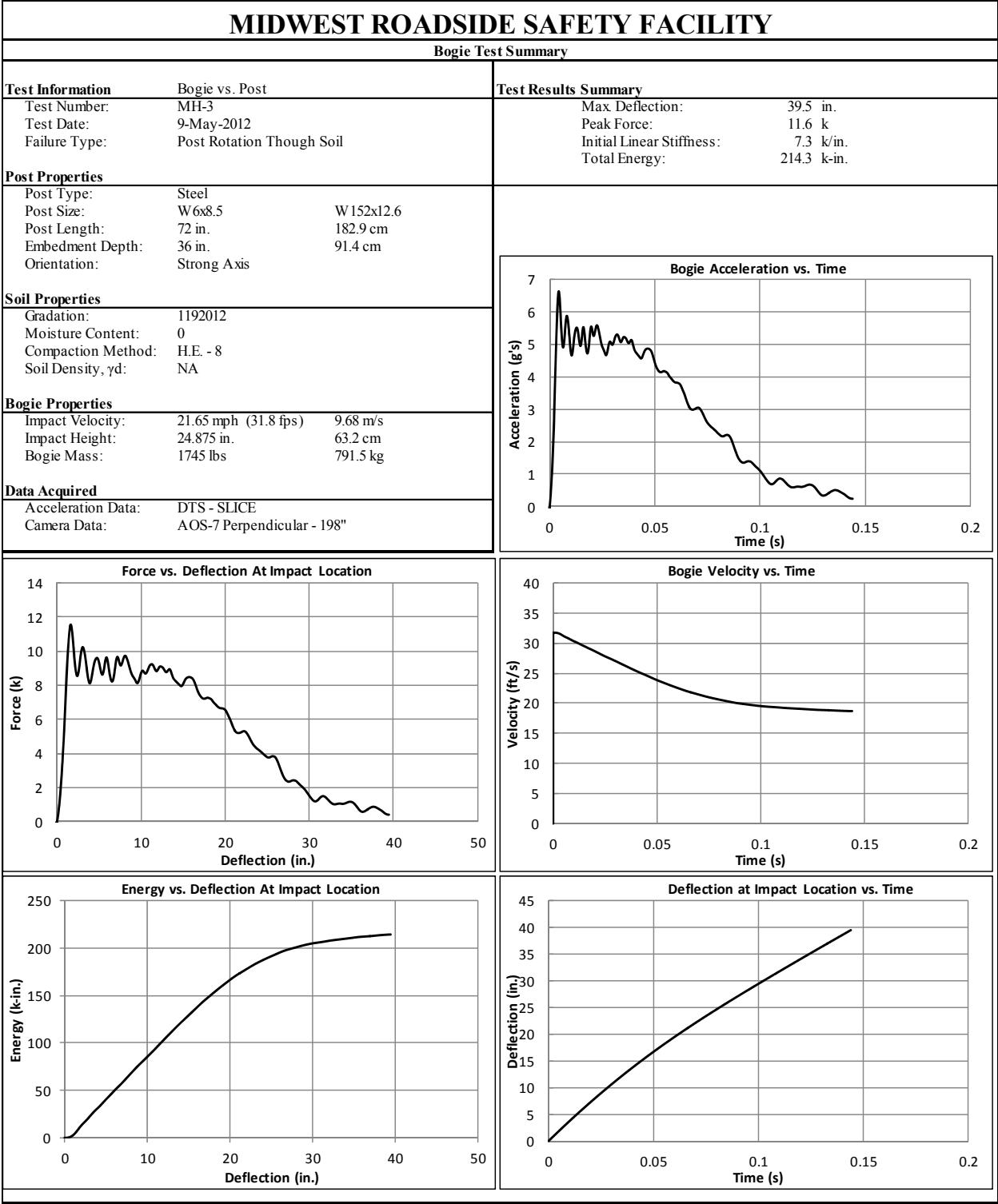


Figure C-5. Test No. MH-3 Results (DTS SLICE)

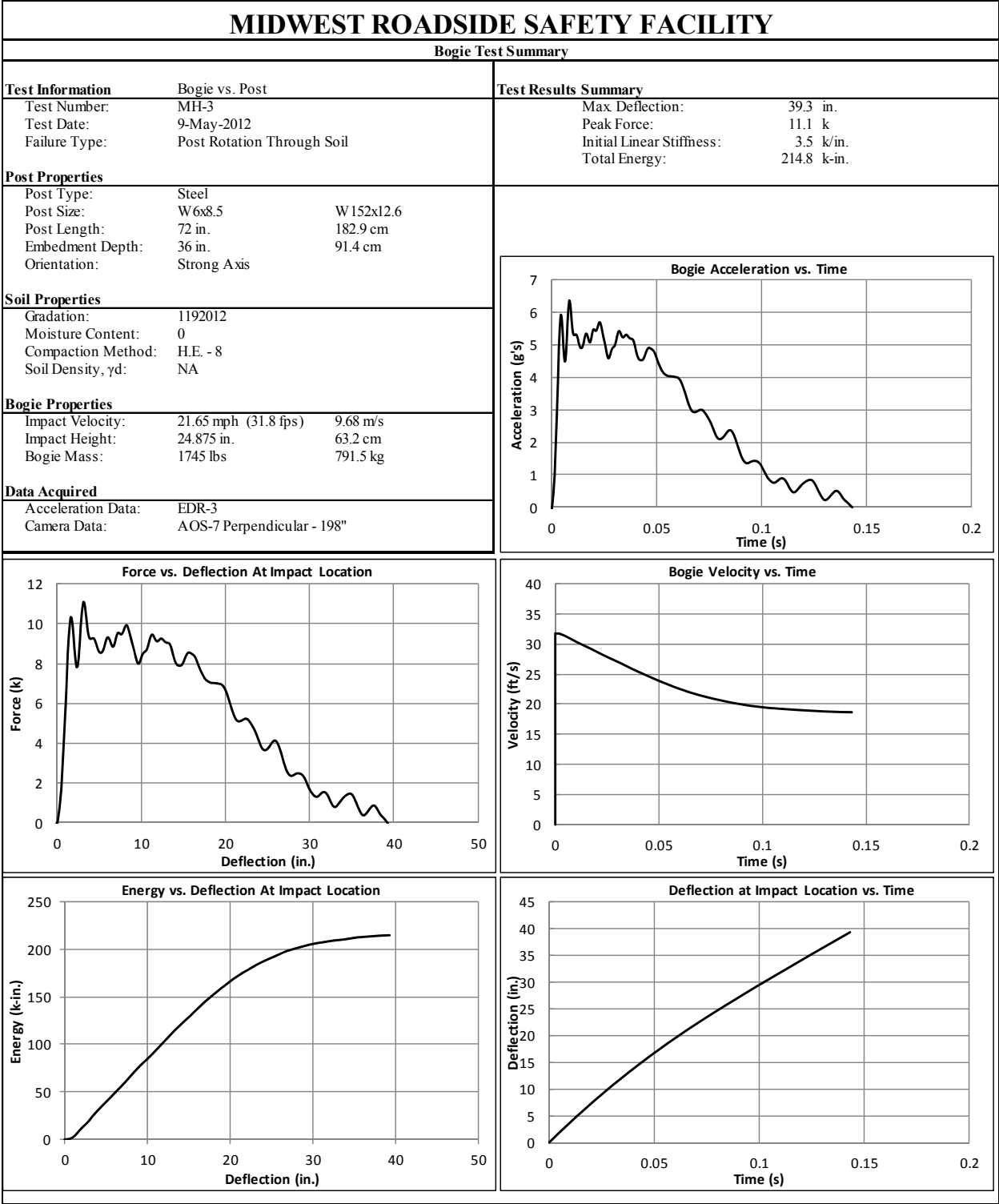


Figure C-6. Test No. MH-3 Results (EDR-3)

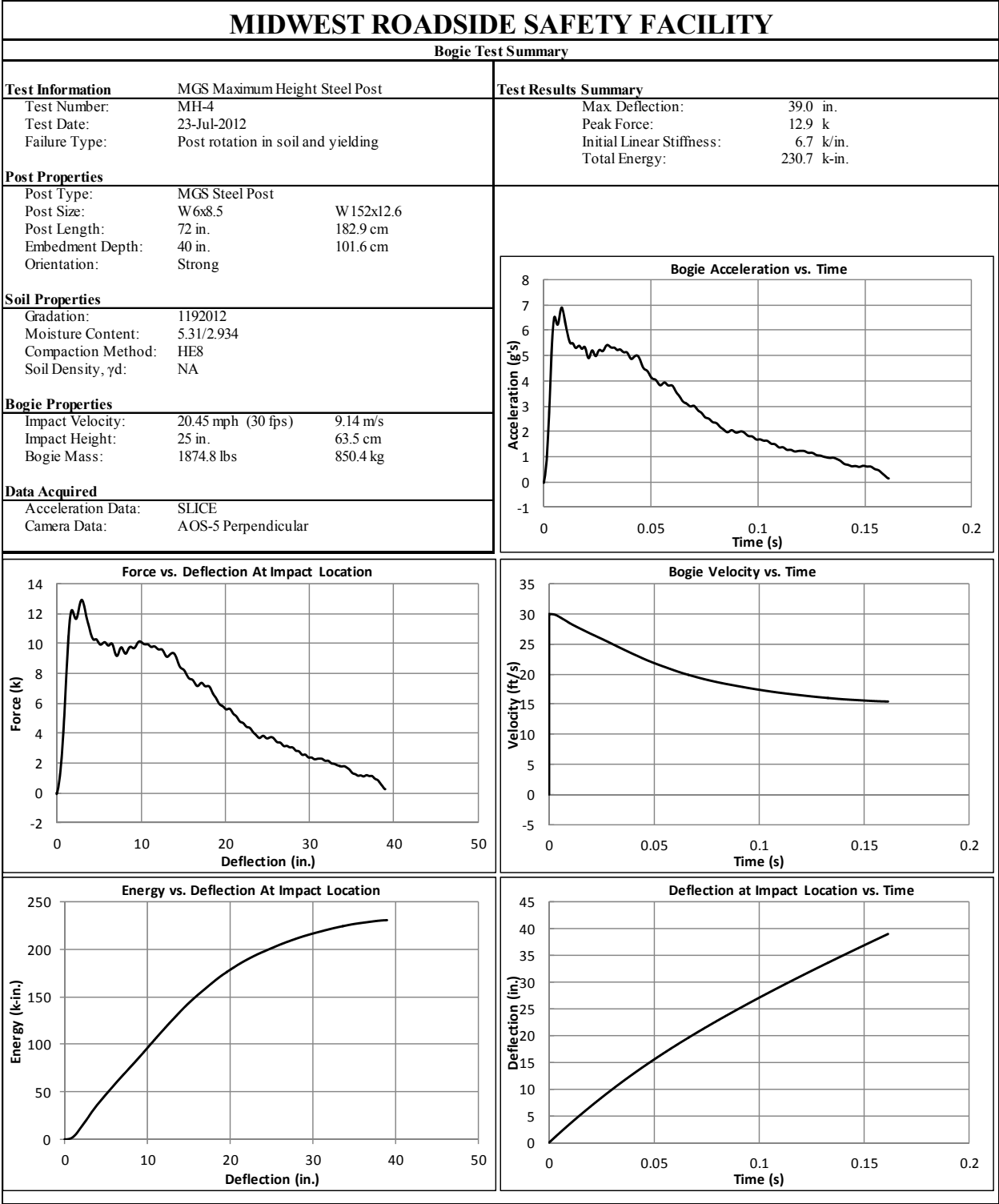


Figure C-7. Test No. MH-4 Results (DTS SLICE)

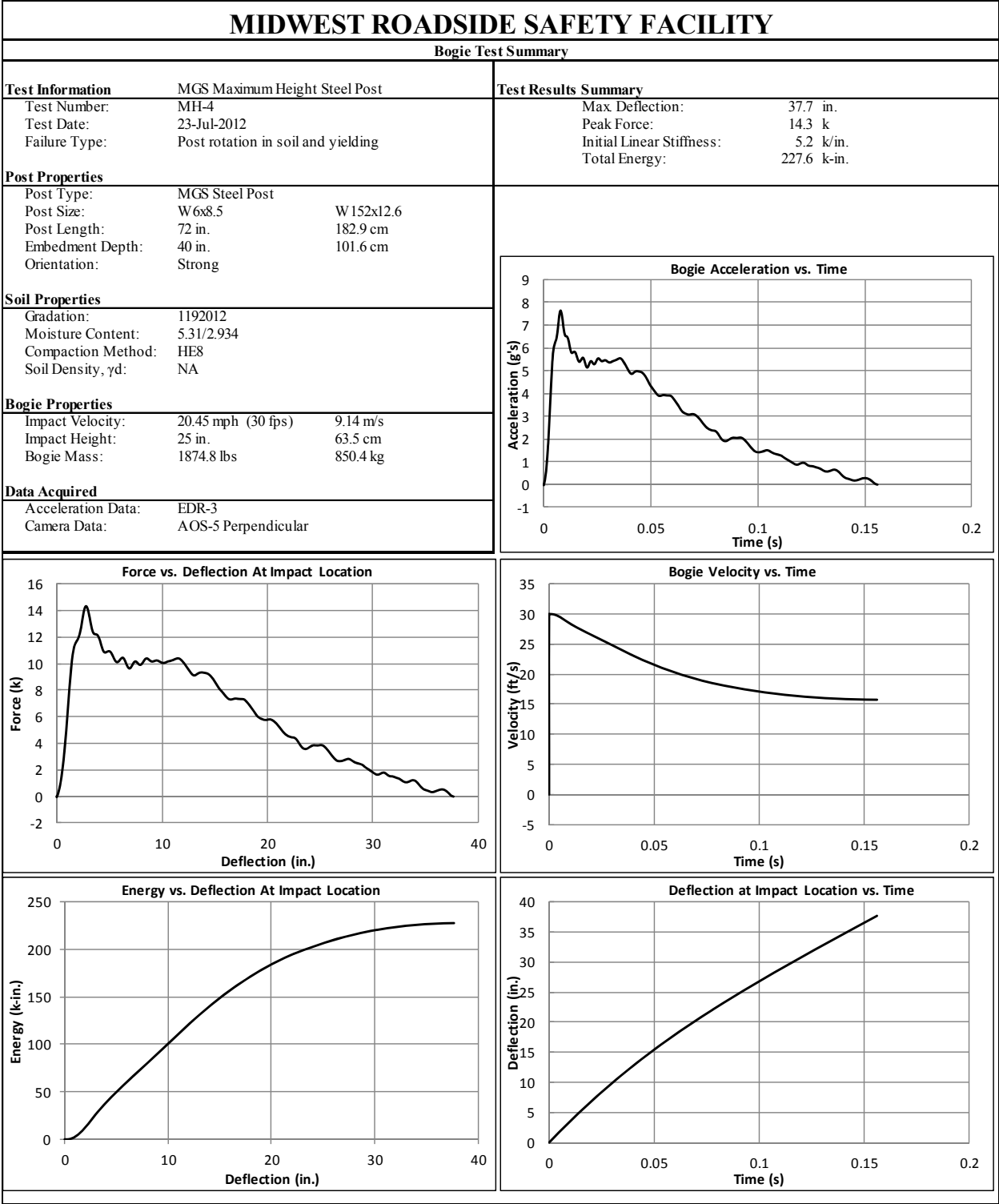


Figure C-8. Test No. MH-4 Results (EDR-3)



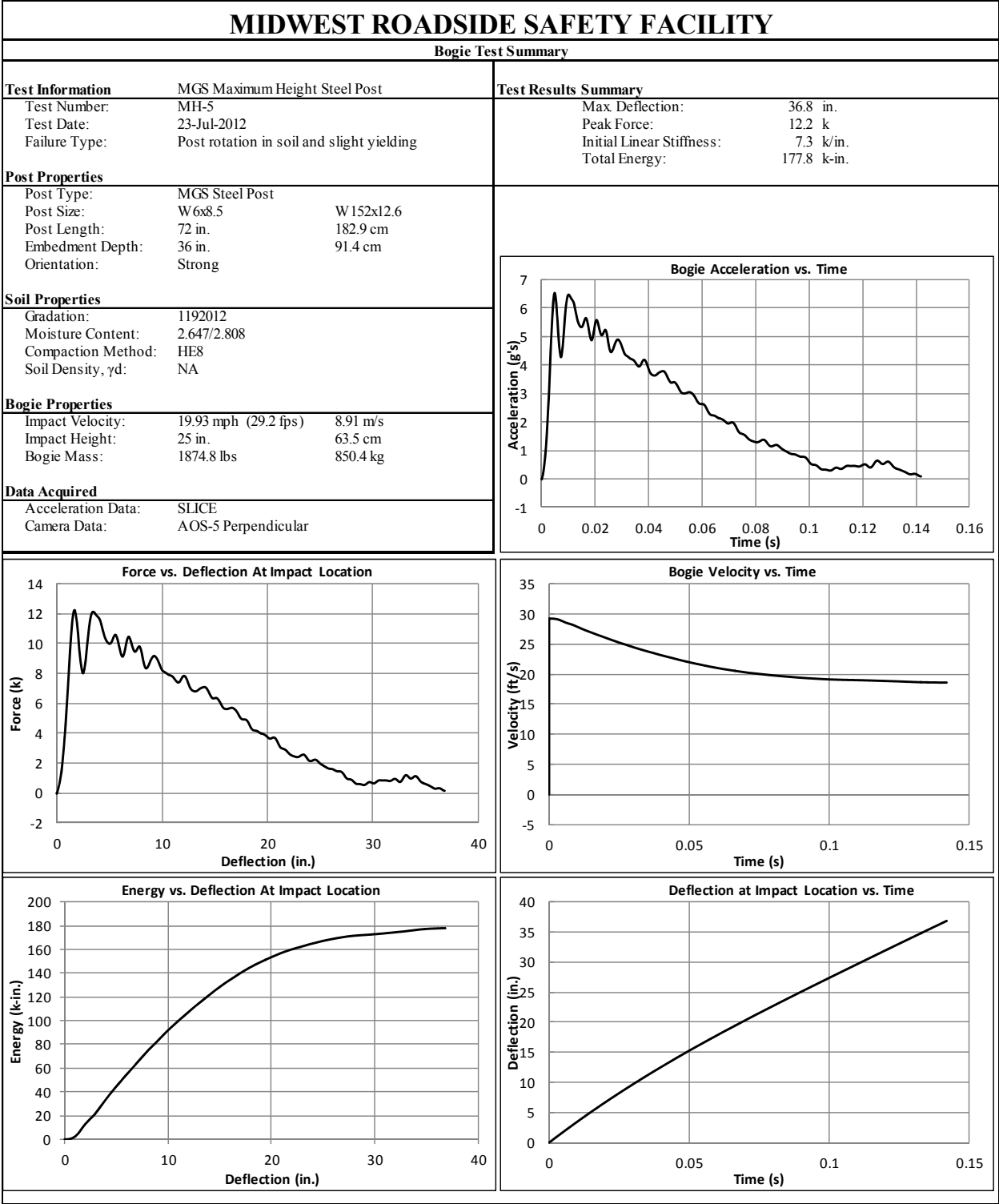


Figure C-9. Test No. MH-5 Results (DTS SLICE)

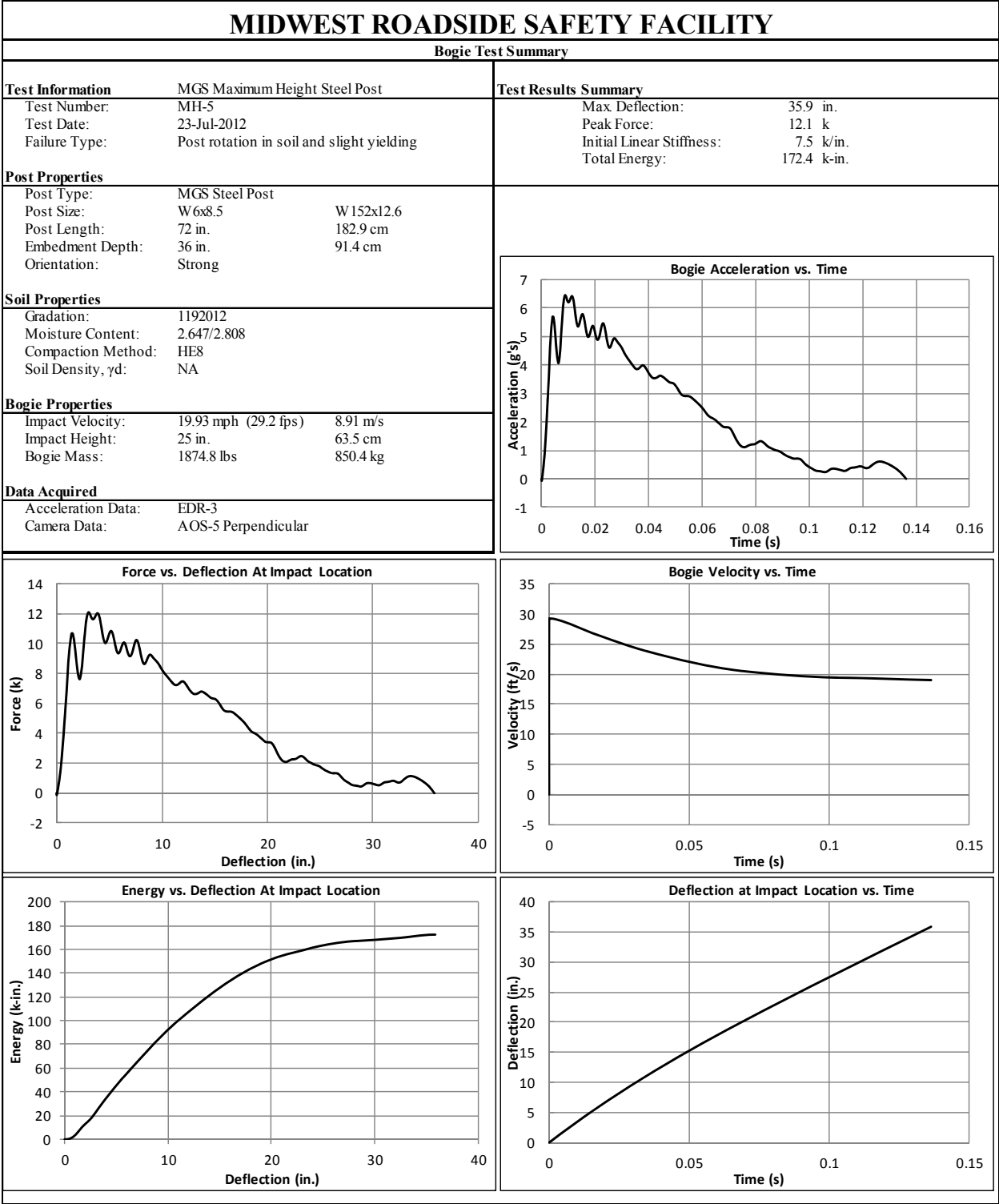


Figure C-10. Test No. MH-5 Results (EDR-3)

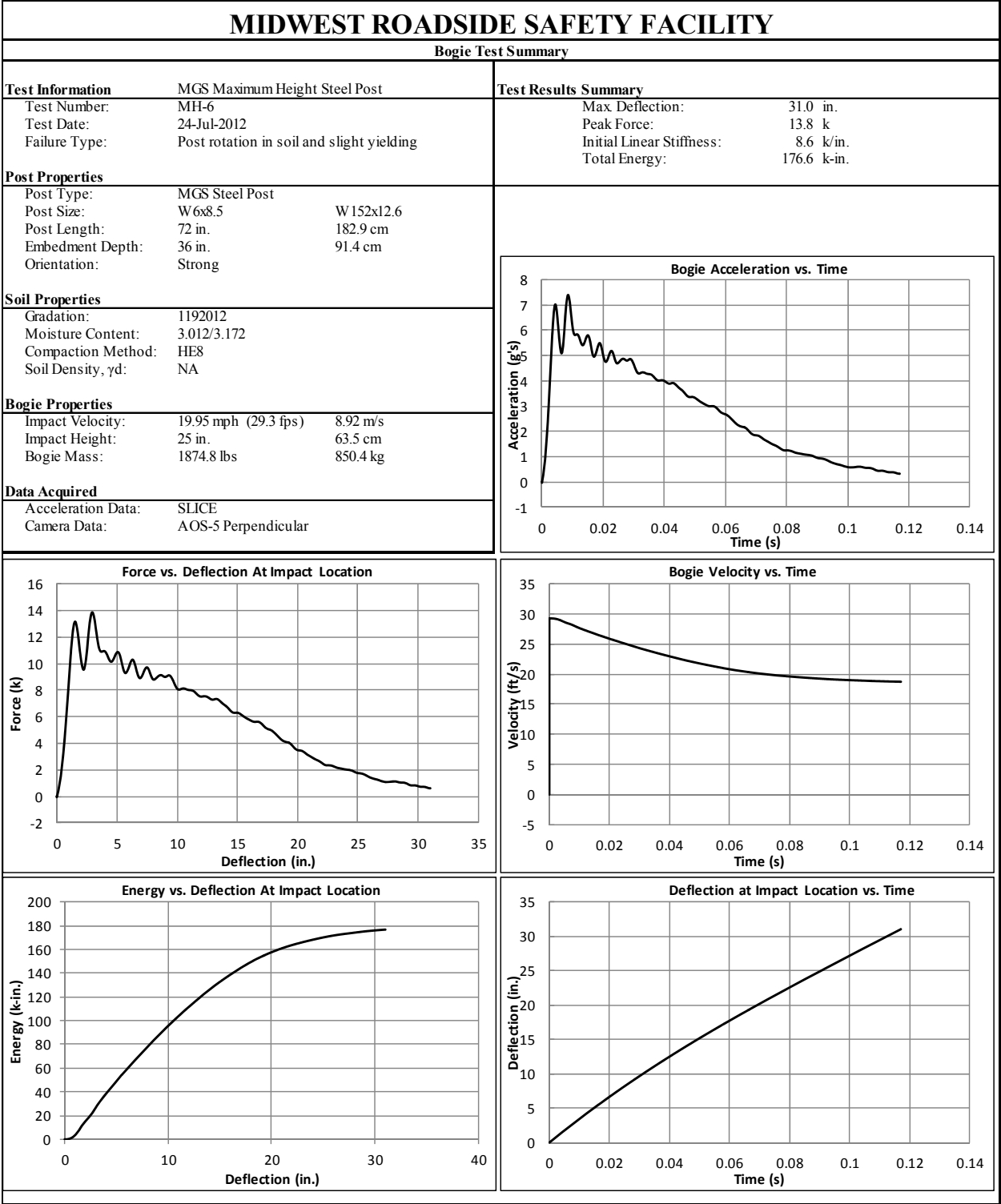


Figure C-11. Test No. MH-6 Results (DTS SLICE)

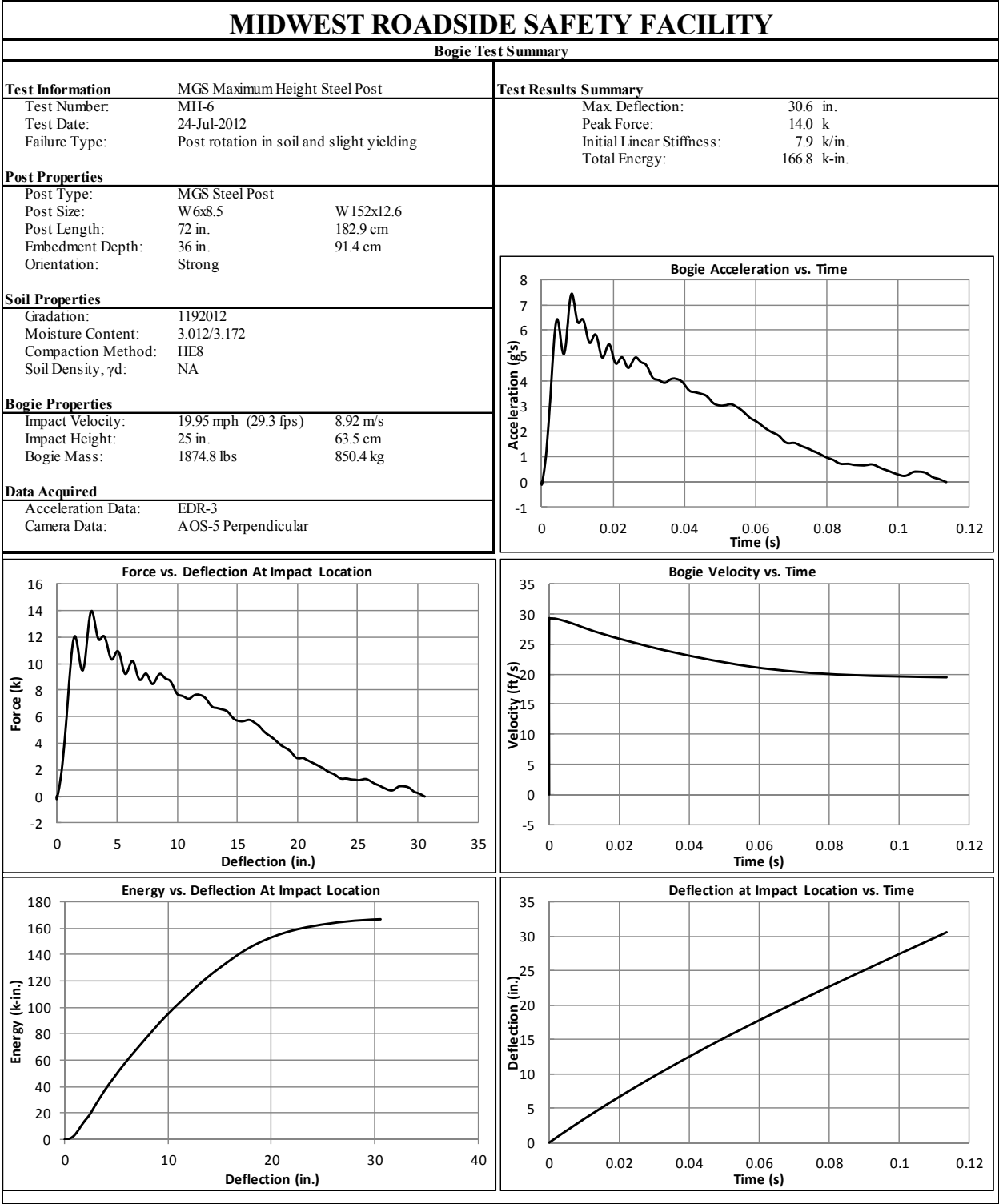


Figure C-12. Test No. MH-6 Results (EDR-3)

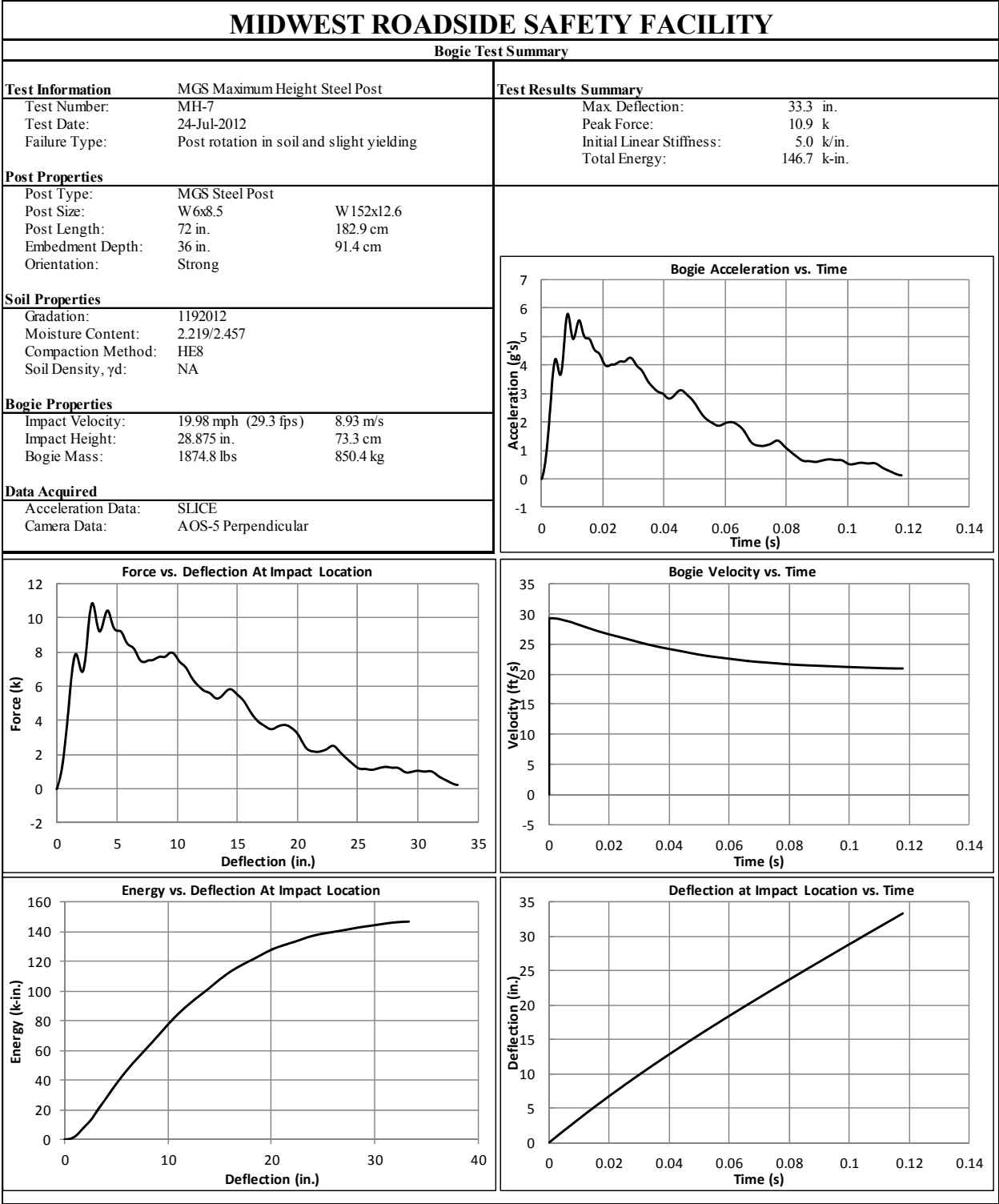


Figure C-13. Test No. MH-7 Results (DTS SLICE)

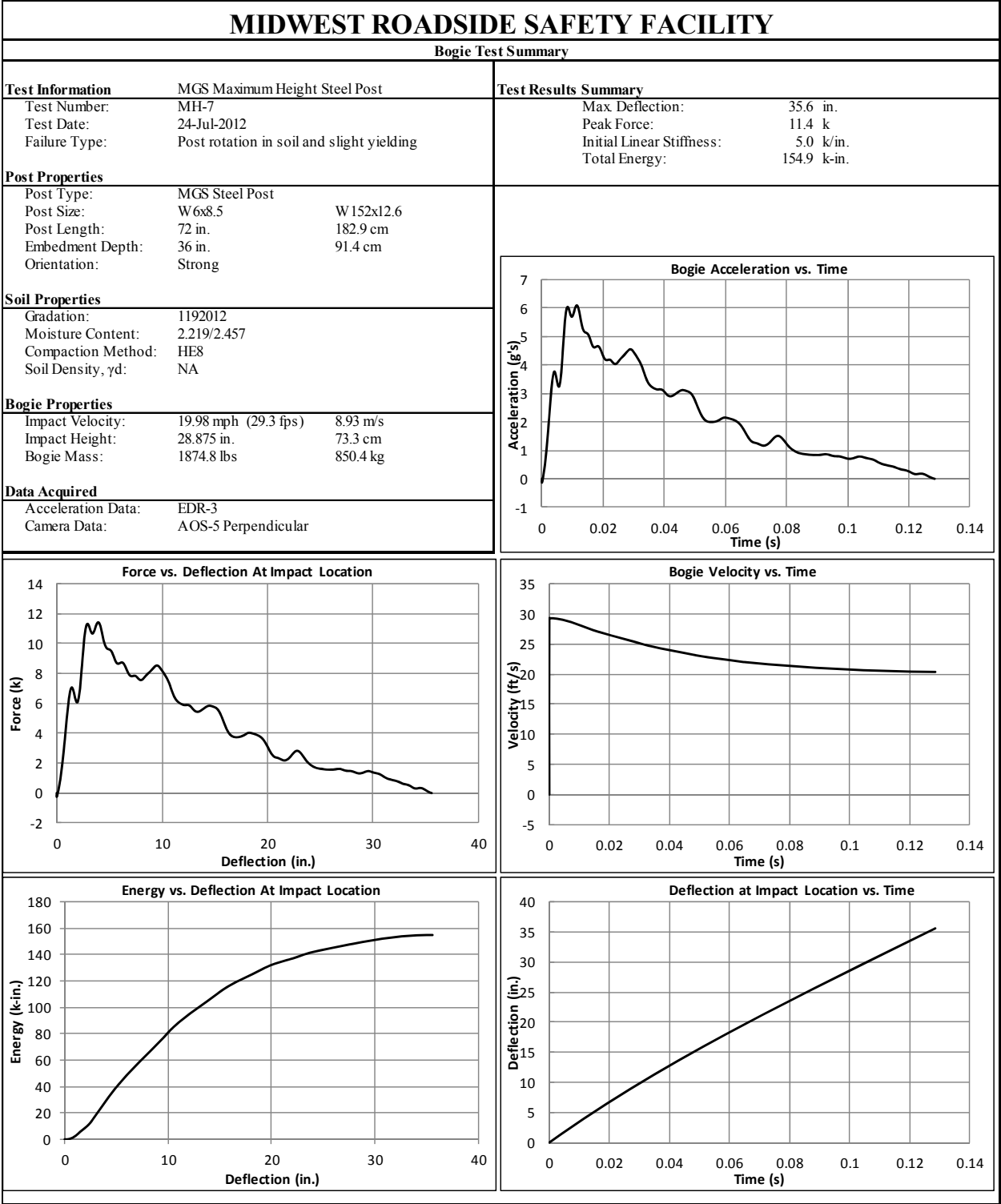


Figure C-14. Test No. MH-7 Results (EDR-3)

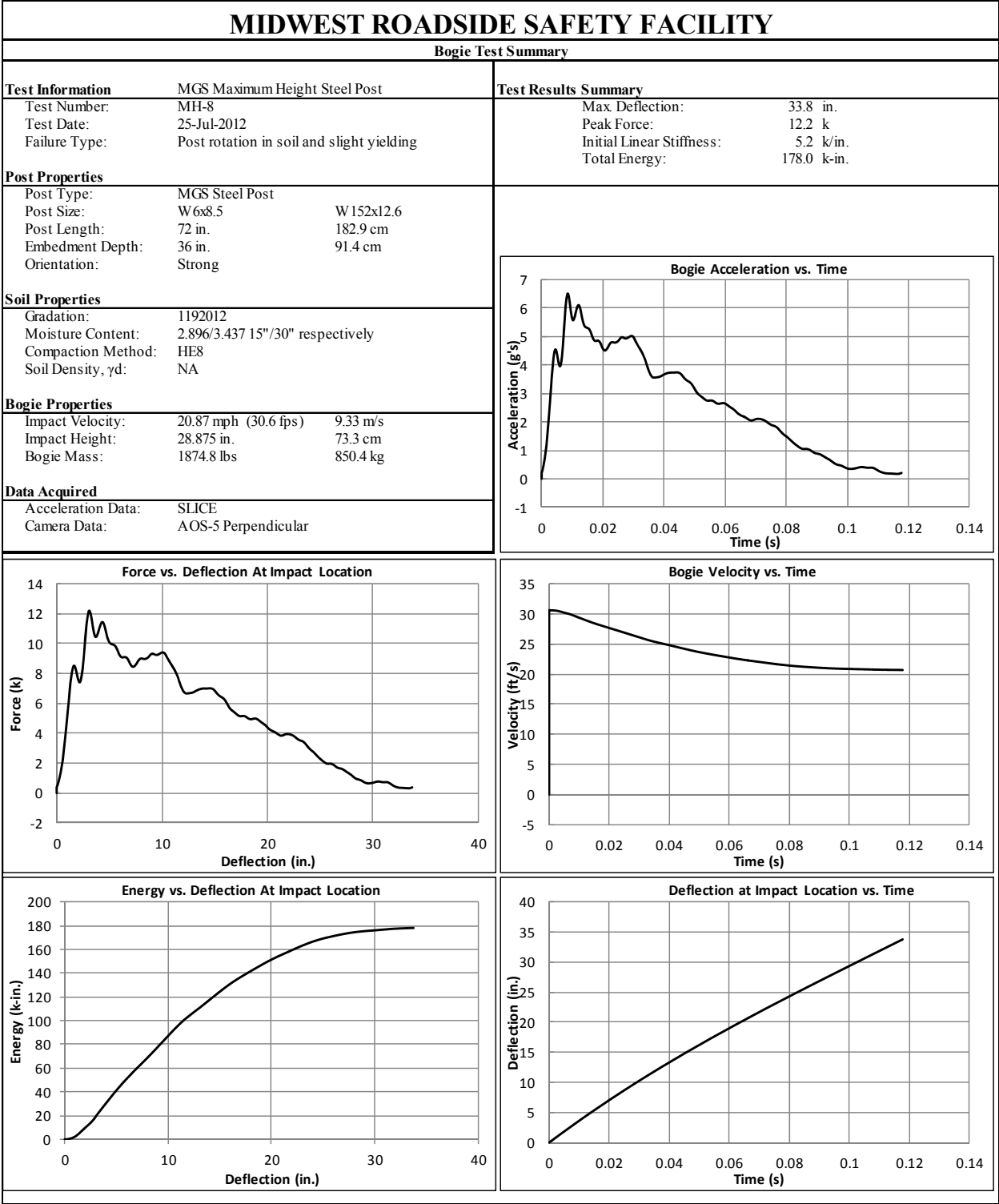


Figure C-15. Test No. MH-8 Results (DTS SLICE)

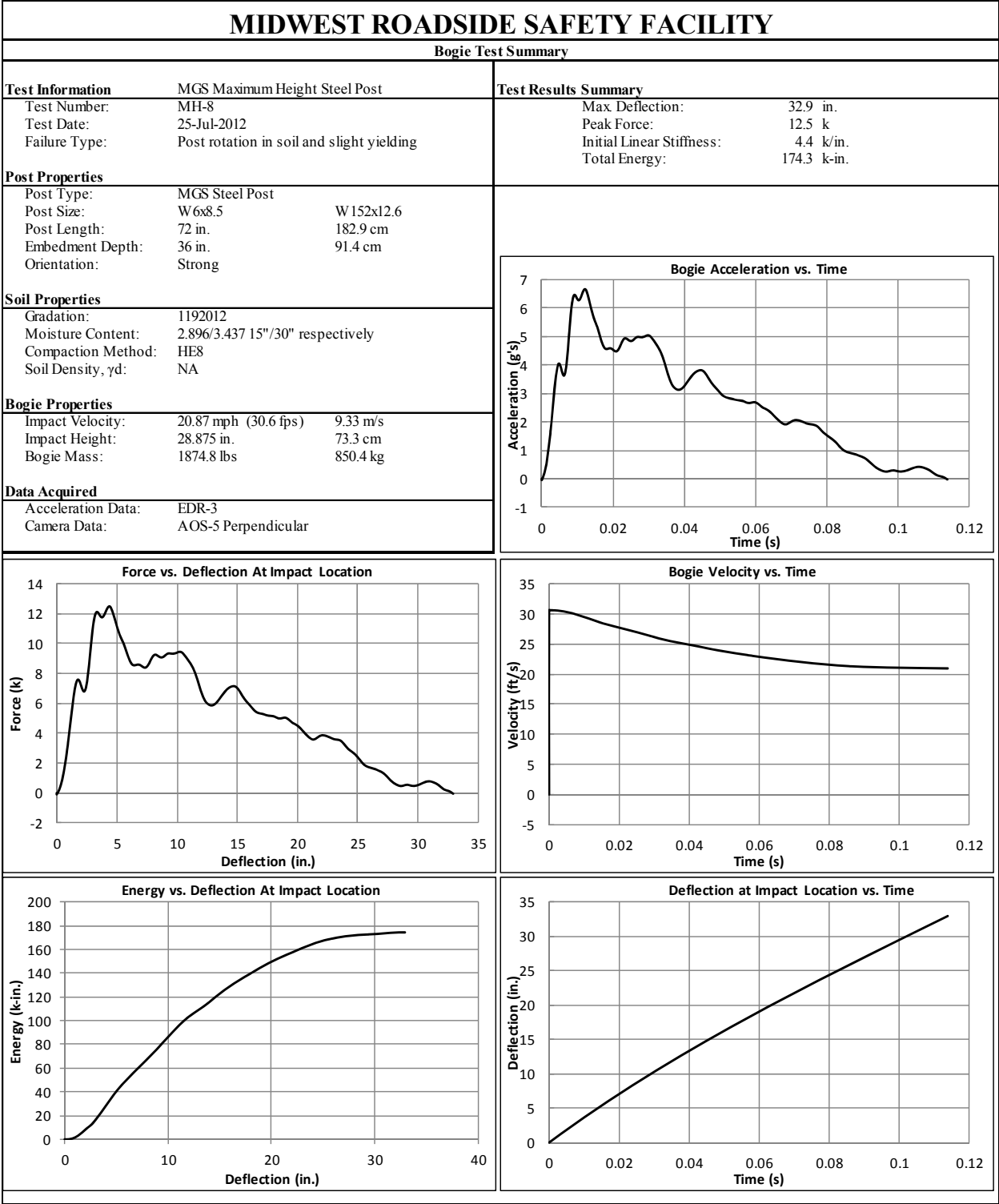


Figure C-16. Test No. MH-8 Results (EDR-3)



**END OF DOCUMENT**